TECHNICAL PAPER

Vibration analysis of rotating cross-ply laminated cylindrical, conical and spherical shells by using weak-form differential quadrature method

Poknam Han[1] · Kwangchol Ri[2] · Kwangnam Choe[2] · Yongnam Han[2]

Abstract

In this article, the weak-form differential quadrature method is adopted to analyze the vibration characteristics of rotating laminated thin shells with arbitrary boundary conditions. Firstly, based on the Reissner–Naghdi's linear shell theory, the energy expression of rotating laminated cylindrical, conical and spherical shells is established. The arbitrary boundary conditions are simulated equivalently by introducing the boundary spring. According to the energy method, the numerical differentiation and numerical integration techniques of the differential quadrature method are combined into the Ritz method, where the admissible function is not introduced in the whole solution process, so to obtain the displacement of any point in the element, it is necessary to use the polynomial to approximate the admissible function of shell. In this paper, the Lagrangian interpolation polynomials are used. The correctness of the current solution model is fully proved by a series of numerical examples. On this basis, the vibration characteristics of rotating cross-ply laminated cylindrical, conical and spherical shells under elastic boundary conditions are further studied.

1 Introduction

The rotating shell structure, as a basic component, has been widely used in gas turbine drive shaft, high-speed centrifugal separator, high-power jet engine, motor and rotor system and other engineering structures. Moreover, such a structure has widely exploited composite material during the past decade. In practical engineering, the rotating shells are subjected to the complex and diverse boundary conditions, and hence, their vibration characteristics are very important and significant in their structural design. In this paper, a unified modeling and its vibration analysis for cylindrical, conical and spherical shells with a general elastic boundary condition were conducted. Many researches on the vibration characteristics of rotating cylindrical, conical and spherical shells have been already conducted.

Lam and Loy [1] studied the free vibration of thin rotating laminated composite cylindrical shells with simply supported and investigated the effect of several parameters on the frequency characteristics. Hua and Lam [2] studied the effects of boundary conditions on frequency characteristics of a thin rotating cylindrical shell by using the generalized differential quadrature (GDQ) method and Love-type shell theory. Lee and Kim [3] studied the free vibrations of simply supported rotating composite cylindrical shells with orthogonal stiffeners. Liew et al. [4] applied the harmonic reproducing kernel particle method for free vibration analysis of rotating cylindrical shells with classical boundary conditions. Saito and Endo [5] used the Galerkin's method to study the vibration behavior of rotating cylindrical shell with three kinds of boundary conditions including clamped, simply supported without axial constraint and simply supported with axial constraint. Civalek and Gürses [6] studied

---

Technical Editor: Thiago Ritto.

✉ Kwangchol Ri
    RKC_1979@163.com

1   College of Ship and Ocean Technology, Kim Chaek University of Technology, Pyongyang 999093, Democratic People's Republic of Korea

2   Department of Light Industry Machinery Engineering, Pyongyang University of Mechanical Engineering, Pyongyang 999093, Democratic People's Republic of Korea

the free vibration of rotating cylindrical shells with classical boundary conditions by using the discrete singular convolution technique. Malekzadeh and Heydarpour [7] used the differential quadrature method to study the free vibration of rotating functionally graded cylindrical shells in thermal environment. Daneshjou and Talebitooti [8] studied the free vibration of rotating stiffened composite cylindrical shells using layerwise-differential quadrature (LW-DQ) method. Song et al. [9] applied the Rayleigh–Ritz method to study the traveling wave of rotating cross-ply laminated cylindrical shells with arbitrary boundary conditions. Cai [10] studied the free vibration of truncated conical shells using discrete variable method. Lam and Li [11] studied the free vibration of rotating truncated circular orthotropic conical shell with simply supported. Civalek [12] extended the discrete singular convolution method to study the free vibration of rotating conical shells with classical boundary conditions. Talebitooti [13] used layerwise-differential quadrature (LW-DQ) method to study three-dimensional free vibration of rotating laminated conical shells. Heydarpour et al. [14] studied vibration behavior of rotating functionally graded carbon nanotube-reinforced composite truncated conical shells with classical boundary conditions by using the differential quadrature method. Dai et al. [15] investigated the free vibration of rotating truncated conical shells using the Haar wavelet method. Talebitooti [16] used Galerkin's method to investigate the influence of thermal effect on free vibration of ring-stiffened rotating functionally graded conical shell with clamped boundary conditions. Tornabene [17] applied the generalized differential quadrature for evaluation of the critical speed of rotating doubly curved multilayered shell structures. Compared with the rotating cylindrical and conical shells, the relevant literature on the vibration characteristics of rotating spherical shells has not been published.

The most commonly used methods are the differential quadrature method, discrete singular convolution method, Rayleigh–Ritz method and so on. Of course, in addition to them, there are also many excellent numerical methods that can be used to deal with such problems, for example, the variational iteration method and the homotopy perturbation method. Homotopy analysis method (HAM) was first proposed by Liao [18]. Unlike the perturbative and non-perturbative methods, this technique allows more than a uniformly valid analytic solution of nonlinear equations with no possible small parameters. Variational iteration method was first proposed by He [19]. In this method, the problems are initially approximated with possible unknowns. Then, a correction functional is constructed by a general Lagrange multiplier, which can be identified optimally via the variational theory. Being different from the other nonlinear analytical methods, like perturbation methods, this method does not depend on small parameters, such that it can find wide application in nonlinear problems without linearization or small perturbations. Although the above methods can be applied to solve the problems in this paper, they are more complex and need a better mathematical basis. However, limited to the author's own level, in this paper, the author will adopt a differential quadrature method in the form of weak solutions. At present, there are two types of DQM, that is, the strong-form DQM and weak-form DQM. Among them, the weak-form DQM is more flexible and more accurate than the strong-form DQM, so it has been widely used in the interpretation of structural mechanics [20, 21].

Through the detailed review above, it can be found that most of the current research on rotating laminated cylindrical, conical and spherical shells is for a single structure, and a unified vibration characteristic analysis model has never been established. For boundaries, due to the limitations of research methods, most of the boundary conditions studied are confined to classical boundary conditions. In addition, the research on the vibration characteristics of rotating spherical shells has not been published. Based on this background, it is very urgent and significant to carry out the research described in the title. The main research objects of this paper contain rotating laminated cylindrical, conical and spherical shells. All energy equations are based on Reissner–Naghdi's linear shell theory. The general elastic boundary conditions are obtained by means of boundary springs. The vibration characteristics of rotating laminated cylindrical, conical and spherical shells are solved by using WDQM, and the correctness of the model is verified by comparing the existing literature results with the finite element simulation results. Finally, this paper also presents a series of unpublished numerical results and conclusions for the first time, which can be used as comparative data for future research in this field.

2 Theoretical formulations

2.1 Description of rotating shells

Figure 1 shows the rotating laminated cylindrical shell, conical shell and spherical shell rotating at angular velocity Ω (rad/s) around their symmetrical axes. Figure 2 shows the coordinate system of cylindrical, conical and spherical shells. The deformation displacements of the rotating shell with respect to the coordinate system can be defined by u, v and w in the α, β and z directions, respectively. As described earlier, three groups of linear springs and one group of rotating spring are introduced at the boundary to simulate the boundary force, and then, corresponding boundary conditions are obtained, as shown in Fig. 1.
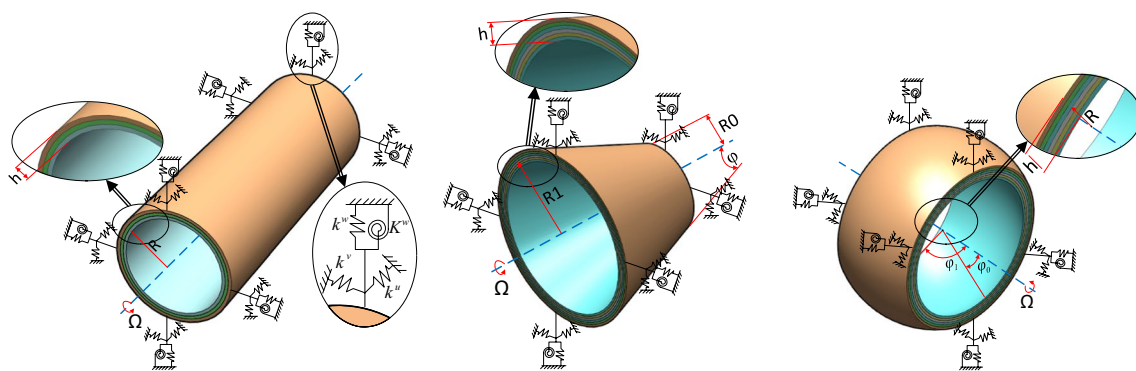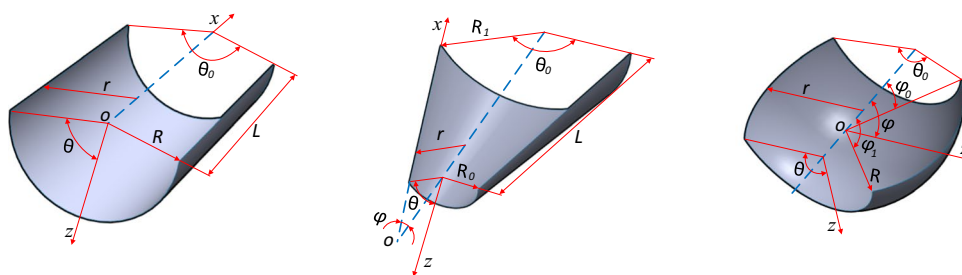
Fig. 1 Rotating laminated composite shell with elastic boundary

Fig. 2 Coordinate system of the cylindrical, conical and spherical shells

2.2 Differential quadrature principle

The relevant principles of DQM have been fully explained [22, 23]. However, in order to make readers have a better understanding of it, the principle of the differential solution will be briefly described before carrying out the research. In addition, because the rotating shell considered in this paper is axially symmetrical, the differential quadrature is only introduced in the axial direction, so the principle of one-dimensional differential quadrature is mainly introduced below. According to the existing research results of the differential quadrature, the kth derivative of a field variable $f(x)$ at point x_i can be expressed by a weighted linear sum as [24, 25]:

$$f_i^{(k)} = \sum_{j=1}^{N} A_{ij}^{(k)} f_j \quad (i = 1, 2, \ldots, N) \text{ or } f_i^{(k)}$$
$$= \mathbf{A}^{(k)} \mathbf{f} \rightarrow \mathbf{f} = \left[f_1 f_2 \ldots f_N \right]^T \tag{1}$$

where $A_{ij}^{(k)}$ are the weighting coefficients of the kth-order derivatives and N is the number of grid points in the x-direction. The specific expression of the weight coefficient can be expressed as follows:

$$\mathbf{A}^{(k)} = \begin{bmatrix} A_{11}^{(k)} & A_{12}^{(k)} & \cdots & A_{1N}^{(k)} \\ A_{21}^{(k)} & A_{22}^{(k)} & \cdots & A_{2N}^{(k)} \\ \vdots & \vdots & \ddots & \vdots \\ A_{N1}^{(k)} & A_{N2}^{(k)} & \cdots & A_{NN}^{(k)} \end{bmatrix} \tag{2}$$

$$A_{ij}^{(1)} = \frac{\prod_{k=1, k \neq i}^{N} \left(x_i - x_k \right)}{\left(x_i - x_k \right) \prod_{k=1, k \neq j}^{N} \left(x_j - x_k \right)} \tag{3}$$

$$A_{ij}^{(s)} = s \left(A_{ij}^{(s-1)} A_{ij}^{(1)} - \frac{A_{ij}^{(s-1)}}{x_i - x_j} \right) \quad i \neq j, 2 \leq s \leq (N-1) \tag{4}$$

$$A_{ii}^{(s)} = -\sum_{j=1, j \neq i}^{N} A_{ij}^{(s)} \quad 1 \leq s \leq (N-1). \tag{5}$$

In the follow-up study, the Gauss–Lobatto quadrature will be also used. Here, based on the existing literature, a brief introduction is also given. The Gauss–Lobatto quadrature rule [24, 25] with precision degree $(2n-3)$ for function $f(x)$ defined at $[-1, 1]$ is:

$$\int_{-1}^{1} f(\xi)\mathrm{d}x = \sum_{j=1}^{N} C_j f(\xi_j) = \mathbf{C}\mathbf{f} \tag{6}$$

where

$$\mathbf{C} = \begin{bmatrix} C_1 & 0 & \cdots & 0 \\ 0 & C_2 & \cdots & 0 \\ \vdots & \vdots & \ddots & \vdots \\ 0 & 0 & \cdots & C_N \end{bmatrix} C_1 = C_N = \frac{2}{N(N-1)},$$

$$C_j = \frac{2}{N(N-1)\left[P_{N-1}(\xi_j)\right]^2} \; (j \neq 1, N). \tag{7}$$

2.3 Expressions of rotating shell's energy

In this paper, the Reissner–Naghdi's linear shell theory is adopted for modeling. In this way, the displacement variations in the α, β and z directions are expressed by the following linear relationships [26]:

$$u(\alpha, \beta, z) = u_0(\alpha, \beta) + z\phi_\alpha(\alpha, \beta)$$
$$v(\alpha, \beta, z) = v_0(\alpha, \beta) + z\phi_\beta(\alpha, \beta) \tag{8}$$
$$w(\alpha, \beta, z) = w_0(\alpha, \beta)$$

where u_0, v_0, w_0 are the displacement components for the middle surface in α, β and z directions, respectively, and ϕ_α and ϕ_β represent the rotation of transverse normal on β and α axes, respectively.

$$\phi_\alpha = \frac{u}{R_\alpha} - \frac{1}{A}\frac{\partial w}{\partial \alpha} \quad \phi_\beta = \frac{v}{R_\beta} - \frac{1}{B}\frac{\partial w}{\partial \beta} \tag{9}$$

where R_α and R_β are the mean radii of curvature of middle surface in α and β directions, respectively.

The strain–displacement relations of rotating shells can be rewritten as [26]:

$$\varepsilon_\alpha = \frac{\partial u}{\partial \alpha} = \varepsilon_\alpha^0 + z\chi_\alpha$$
$$\varepsilon_\beta = \frac{\partial v}{\partial \beta} = \varepsilon_\beta^0 + z\chi_\beta \tag{10}$$
$$\gamma_{\alpha\beta} = \frac{\partial u}{\partial \beta} + \frac{\partial v}{\partial \alpha} = \gamma_{\alpha\beta}^0 + z\chi_{\alpha\beta}$$

where ε_α^0, ε_β^0, $\gamma_{\alpha\beta}^0$ represent the normal strain and shear strain for middle surface and χ_α, χ_β, $\chi_{\alpha\beta}$ denote the corresponding curvature and twist changes.

$$\varepsilon_\alpha^0 = \frac{1}{A}\frac{\partial u}{\partial \alpha} + \frac{v}{AB}\frac{\partial A}{\partial \beta} + \frac{w}{R_\alpha} \tag{11a}$$

$$\varepsilon_\beta^0 = \frac{1}{B}\frac{\partial v}{\partial \beta} + \frac{u}{AB}\frac{\partial B}{\partial \alpha} + \frac{w}{R_\beta} \tag{11b}$$

$$\gamma_{\alpha\beta}^0 = \frac{1}{A}\frac{\partial v}{\partial \alpha} - \frac{u}{AB}\frac{\partial A}{\partial \beta} + \frac{1}{B}\frac{\partial u}{\partial \beta} - \frac{v}{AB}\frac{\partial B}{\partial \alpha} \tag{11c}$$

$$\chi_\alpha = \frac{1}{A}\frac{\partial \phi_\alpha}{\partial \alpha} + \frac{\phi_\beta}{AB}\frac{\partial A}{\partial \beta} \tag{11d}$$

$$\chi_\beta = \frac{1}{B}\frac{\partial \phi_\beta}{\partial \beta} + \frac{\phi_\alpha}{AB}\frac{\partial B}{\partial \alpha} \tag{11e}$$

$$\chi_{\alpha\beta} = \frac{1}{A}\frac{\partial \phi_\beta}{\partial \alpha} - \frac{\phi_\alpha}{AB}\frac{\partial A}{\partial \beta} + \frac{1}{B}\frac{\partial \phi_\alpha}{\partial \beta} - \frac{\phi_\beta}{AB}\frac{\partial B}{\partial \alpha} \tag{11f}$$

where A and B are the Lamé parameters.

It must be noted here that, according to different structural forms, there are specific differences in the coordinate system forms. Therefore, the specific variables represented by the symbolic variables also have certain differences, which can be expressed as follows [26]:

$$\text{Cylindrical shell}: \; \alpha = x \quad \beta = \theta \quad R_\alpha = \infty \quad R_\beta = R$$
$$A = 1 \quad B = R$$
$$\text{Conical shell}: \; \alpha = x \quad \beta = \theta \quad R_\alpha = 1 \quad R_\beta = x\tan\varphi$$
$$A = 1 \quad B = x\sin\varphi \tag{12}$$
$$\text{Spherical shell}: \; \alpha = \varphi \quad \beta = \theta \quad R_\alpha = R \quad R_\beta = R$$
$$A = R \quad B = R\sin\varphi.$$
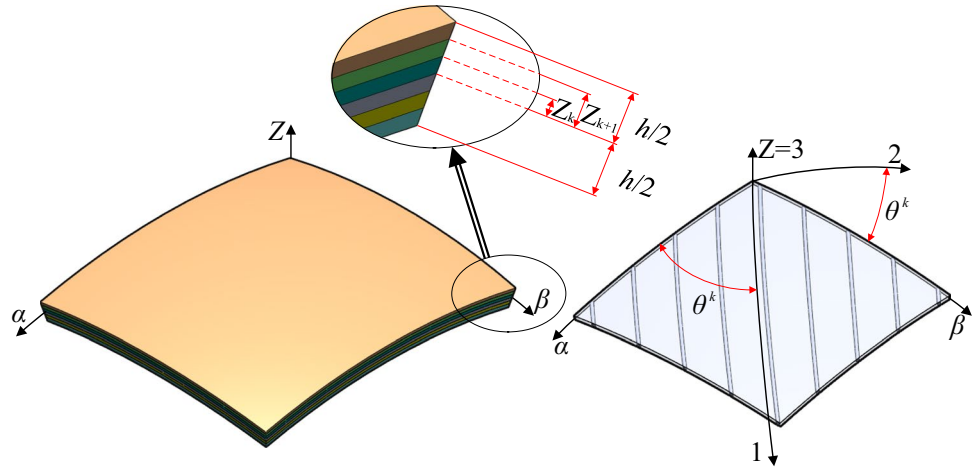
Figure 2 shows each coordinate system in detail.

According to the principle of differential quadrature, the expressions in Eq. (11) can be further expressed as follows:

$$\varepsilon_\alpha^0 = \left[\frac{\mathbf{A}^{(1)}}{A} \; \mathbf{0} \; \frac{\mathbf{E}}{R_\alpha} \right] \begin{bmatrix} \mathbf{U} \\ \mathbf{V} \\ \mathbf{W} \end{bmatrix} \tag{13a}$$

$$\varepsilon_\beta^0 = \left[\frac{1}{AB}\frac{\partial B}{\partial \alpha}\mathbf{E} \; \frac{\mathbf{B}^{(1)}}{B} \; \frac{\mathbf{E}}{R_\beta} \right] \begin{bmatrix} \mathbf{U} \\ \mathbf{V} \\ \mathbf{W} \end{bmatrix} \tag{13b}$$

$$\gamma_{\alpha\beta}^0 = \left[\frac{\mathbf{B}^{(1)}}{B} \; \frac{\mathbf{A}^{(1)}}{A} - \frac{1}{AB}\frac{\partial B}{\partial \alpha}\mathbf{E} \; \mathbf{0} \right] \begin{bmatrix} \mathbf{U} \\ \mathbf{V} \\ \mathbf{W} \end{bmatrix} \tag{13c}$$

Fig. 3 Schematic diagram of the laminated material

$$\chi_\alpha = \left[\begin{array}{ccc} \frac{1}{AR_\alpha}\mathbf{A}^{(1)} & \mathbf{0} & -\frac{\mathbf{A}^{(2)}}{A^2} \end{array} \right] \left[\begin{array}{c} \mathbf{U} \\ \mathbf{V} \\ \mathbf{W} \end{array} \right] \tag{13d}$$

$$\chi_\beta = \left[\begin{array}{ccc} \frac{1}{ABR_\alpha}\frac{\partial B}{\partial \alpha}\mathbf{E} & \frac{1}{BR_\beta}\mathbf{B}_1^{(1)} & -\frac{1}{B^2}\mathbf{B}_1^{(2)} - \frac{1}{A^2B}\frac{\partial B}{\partial \alpha}\mathbf{A}_1^{(1)} \end{array} \right] \left[\begin{array}{c} \mathbf{U} \\ \mathbf{V} \\ \mathbf{W} \end{array} \right] \tag{13e}$$

$$\chi_{\alpha\beta} = \left[\begin{array}{ccc} \frac{1}{BR_\alpha}\mathbf{B}_1^{(1)} & \mathbf{D} - \frac{1}{ABR_\beta}\frac{\partial B}{\partial \alpha}\mathbf{E} & -2\mathbf{F}_1^{(2)} + \frac{1}{AB^2}\frac{\partial B}{\partial \alpha}\mathbf{B}_1^{(1)} \end{array} \right] \left[\begin{array}{c} \mathbf{U} \\ \mathbf{V} \\ \mathbf{W} \end{array} \right] \tag{13f}$$

where $\mathbf{D}$ is given according to the value of R_β, $\mathbf{A}^{(1)}$, $\mathbf{B}^{(1)}$, $\mathbf{A}^{(2)}$, $\mathbf{B}_1^{(1)}$, $\mathbf{B}_1^{(2)}$, $\mathbf{F}_1^{(2)}$ are weighting coefficients. $\mathbf{U}$, $\mathbf{V}$ and $\mathbf{W}$ are displacement variables. $\mathbf{E}$ and $\mathbf{0}$ are the identity matrix and zero matrix, respectively. The specific expressions will be given in detail later.

$$\left\{ \begin{array}{c} \sigma_\alpha \\ \sigma_\beta \\ \tau_{\alpha\beta} \end{array} \right\}_k = \left[\begin{array}{ccc} \overline{Q_{11}^k} & \overline{Q_{12}^k} & \overline{Q_{16}^k} \\ \overline{Q_{12}^k} & \overline{Q_{22}^k} & \overline{Q_{26}^k} \\ \overline{Q_{16}^k} & \overline{Q_{26}^k} & \overline{Q_{66}^k} \end{array} \right] \left\{ \begin{array}{c} \varepsilon_\alpha \\ \varepsilon_\beta \\ \gamma_{\alpha\beta} \end{array} \right\}_k ,$$

$$\left[\begin{array}{ccc} \overline{Q_{11}^k} & \overline{Q_{12}^k} & \overline{Q_{16}^k} \\ \overline{Q_{12}^k} & \overline{Q_{22}^k} & \overline{Q_{26}^k} \\ \overline{Q_{16}^k} & \overline{Q_{26}^k} & \overline{Q_{66}^k} \end{array} \right] = T \left[\begin{array}{ccc} Q_{11}^k & Q_{12}^k & 0 \\ Q_{12}^k & Q_{22}^k & 0 \\ 0 & 0 & Q_{66}^k \end{array} \right] T^T \tag{14a}$$

$$Q_{11}^k = \frac{E_1}{1 - \mu_{12}\mu_{21}}, \quad Q_{12}^k = \frac{\mu_{12}E_2}{1 - \mu_{12}\mu_{21}},$$

$$Q_{22}^k = \frac{E_2}{1 - \mu_{12}\mu_{21}}, \quad Q_{66}^k = G_{12} \tag{14b}$$

$$T = \left[\begin{array}{ccc} \cos^2\theta^k & \sin^2\theta^k & -2\sin\theta^k\cos\theta^k \\ \sin^2\theta^k & \cos^2\theta^k & 2\sin\theta^k\cos\theta^k \\ \sin\theta^k\cos\theta^k & -\sin\theta^k\cos\theta^k & \cos^2\theta^k - \sin^2\theta^k \end{array} \right] \tag{14c}$$

$$\overline{Q_{11}^k} = Q_{11}^k\cos^4\theta^k + (2Q_{12}^k + 4Q_{66}^k)\cos^2\theta^k\sin^2\theta^k + Q_{22}^k\sin^4\theta^k$$

$$\overline{Q_{12}^k} = (Q_{11}^k + Q_{22}^k - 4Q_{66}^k)\cos^2\theta^k\sin^2\theta^k + Q_{12}^k(\cos^4\theta^k + \sin^4\theta^k)$$

$$\overline{Q_{16}^k} = (Q_{11}^k - Q_{12}^k - 2Q_{66}^k)\cos^3\theta^k\sin\theta^k + (Q_{12}^k - Q_{22}^k + 2Q_{66}^k)\cos\theta^k\sin^3\theta^k$$

$$\overline{Q_{22}^k} = Q_{11}^k\sin^4\theta^k + Q_{22}^k\cos^4\theta^k + (2Q_{12}^k + 4Q_{66}^k)\cos^2\theta^k\sin^2\theta^k \tag{14d}$$

$$\overline{Q_{26}^k} = (Q_{11}^k - Q_{12}^k - 2Q_{66}^k)\cos\theta^k\sin^3\theta^k + (Q_{12}^k - Q_{22}^k + 2Q_{66}^k)\cos^3\theta^k\sin\theta^k$$

$$\overline{Q_{66}^k} = Q_{66}^k(\cos^4\theta^k + \sin^4\theta^k) + (Q_{11}^k - 2Q_{12}^k + Q_{22}^k - 2Q_{66}^k)\cos^2\theta^k\sin^2\theta^k.$$

Figure 3 shows the concrete schematic diagram of the laminated material. Based on the existing research results, the corresponding stress–strain relations in the kth layer of the laminated shell can be written as [26]:

σ_α, σ_β are the normal stresses in α and β directions, respectively, and $\tau_{\alpha\beta}$ is the shear stress. $Q_{ij}^k(i, j = 1, 2, 6)$ is the elastic stiffness coefficients in the kth layer. E_1, E_2, G_{12}, μ_{12}, μ_{21} are the engineering constants in the orthotropic axes. θ^k is the fiber angle in composite material.
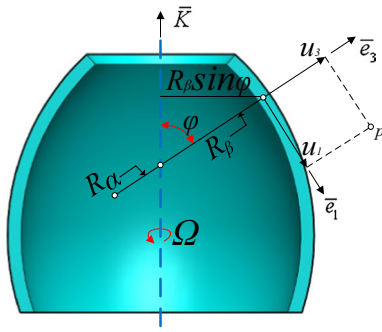
Fig. 4 Coordinate definitions for a general rotating shell

Integrating the stresses over the thickness, the force and moment resultants of thin laminated rotating shells can be obtained in a matrix form as [26]:

$$
\begin{bmatrix} N_\alpha \\ N_\beta \\ N_{\alpha\beta} \\ M_\alpha \\ M_\beta \\ M_{\alpha\beta} \end{bmatrix} = \begin{bmatrix} A_{11} & A_{12} & A_{16} & B_{11} & B_{12} & B_{16} \\ A_{12} & A_{22} & A_{26} & B_{12} & B_{22} & B_{26} \\ A_{16} & A_{26} & A_{66} & B_{16} & B_{26} & B_{66} \\ B_{11} & B_{12} & B_{16} & D_{11} & D_{12} & D_{16} \\ B_{12} & B_{22} & B_{26} & D_{12} & D_{22} & D_{26} \\ B_{16} & B_{26} & B_{66} & D_{16} & D_{26} & D_{66} \end{bmatrix} \begin{bmatrix} \varepsilon_\alpha^0 \\ \varepsilon_\beta^0 \\ \gamma_{\alpha\beta}^0 \\ \chi_\alpha \\ \chi_\beta \\ \chi_{\alpha\beta} \end{bmatrix} \quad (15)
$$

where N_α, N_β and $N_{\alpha\beta}$ are the normal and shear force resultants and M_α, M_β and $M_{\alpha\beta}$ denote the bending and twisting moment resultants. The stiffness coefficients A_{ij}, B_{ij} and D_{ij} are given as:

$$
A_{ij} = \sum_{k=1}^{N} \overline{Q_{ij}^k}(z_{k+1} - z_k), \quad B_{ij} = \frac{1}{2} \sum_{k=1}^{N} \overline{Q_{ij}^k}(z_{k+1}^2 - z_k^2),
$$

$$
D_{ij} = \frac{1}{3} \sum_{k=1}^{N} \overline{Q_{ij}^k}(z_{k+1}^3 - z_k^3). \quad (16)
$$

The strain energy can be divided into three parts [26]:

$$
U_s = \frac{1}{2} \int_\alpha \int_\beta \begin{bmatrix} A_{11}(\varepsilon_\alpha^0)^2 + 2A_{12}\varepsilon_\alpha^0\varepsilon_\beta^0 + A_{22}(\varepsilon_\beta^0)^2 \\ + 2A_{16}\varepsilon_\alpha^0\gamma_{\alpha\beta}^0 + 2A_{26}\varepsilon_\beta^0\gamma_{\alpha\beta}^0 + A_{66}(\gamma_{\alpha\beta}^0)^2 \end{bmatrix} AB\mathrm{d}\alpha\mathrm{d}\beta \quad (17a)
$$

$$
U_c = \frac{1}{2} \int_\alpha \int_\beta 2 \begin{bmatrix} B_{11}\chi_\alpha\varepsilon_\alpha^0 + B_{12}\chi_\beta\varepsilon_\alpha^0 + B_{12}\chi_\alpha\varepsilon_\beta^0 \\ + B_{16}\chi_{\alpha\beta}\varepsilon_\alpha^0 + B_{16}\chi_\alpha\gamma_{\alpha\beta}^0 \\ + B_{22}\varepsilon_\beta^0\chi_\beta + B_{26}\varepsilon_\beta^0\chi_{\alpha\beta} \\ + B_{26}\chi_\beta\gamma_{\alpha\beta}^0 + B_{66}\gamma_{\alpha\beta}^0\chi_{\alpha\beta} \end{bmatrix} AB\mathrm{d}\alpha\mathrm{d}\beta \quad (17b)
$$

$$
U_b = \frac{1}{2} \int_\alpha \int_\beta \begin{bmatrix} D_{11}(\chi_\alpha)^2 + 2D_{12}\chi_\alpha\chi_\beta \\ + D_{22}(\chi_\beta)^2 + 2D_{16}\chi_\alpha\chi_{\alpha\beta} \\ + 2D_{26}\chi_\beta\chi_{\alpha\beta} + D_{66}(\chi_{\alpha\beta})^2 \end{bmatrix} AB\mathrm{d}\alpha\mathrm{d}\beta. \quad (17c)
$$

Figure 4 shows the coordinate definitions for a general rotating shell; the point of interest on the undeformed shell serves as the origin of a moving, right-handed coordinate system defined by the unit vectors $\bar{e}_1$, $\bar{e}_2$ and $\bar{e}_3$ ($\bar{e}_2$ is into the paper). Thus, the particle velocity is [27]:

$$
\bar{v} = \bar{v}_{O'} + (\bar{v}_{P/O'})_{\mathrm{rel}} + \bar{\omega} \times \bar{r}_{P/O'} \quad (18)
$$

where

$$
\begin{aligned} \bar{v}_{O'} &= \Omega R_\theta \sin\varphi\, \bar{e}_2 \\ \bar{\omega} &= \Omega\bar{K} = \Omega\cos\varphi\, \bar{e}_3 - \Omega\sin\varphi\, \bar{e}_1 \\ (\bar{v}_{P/O'})_{\mathrm{rel}} &= \dot{u}\bar{e}_1 + \dot{v}\bar{e}_2 + \dot{w}\bar{e}_3 \\ \bar{r}_{P/O'} &= u\bar{e}_1 + v\bar{e}_2 + w\bar{e}_3 \end{aligned} \quad (19)
$$

where φ is the angle along the meridional direction of shell.

Substituting Eqs. (19) into (18) yields

$$
\begin{aligned} \bar{v} =& (\dot{u} - v\Omega\cos\varphi)\bar{e}_1 + (\Omega R_\beta \sin\varphi + \dot{v} + u\Omega\cos\varphi + w\Omega\sin\varphi)\bar{e}_2 \\ &+ (\dot{w} - v\Omega\sin\varphi)\bar{e}_3. \end{aligned} \quad (20)
$$

The kinetic energy is, therefore,

$$
\begin{aligned} T &= \frac{\rho h}{2} \int_\alpha \int_\beta (\bar{v} \cdot \bar{v}) AB\mathrm{d}\alpha\mathrm{d}\beta \\ &= \frac{\rho h}{2} \int_\alpha \int_\beta \left[(\dot{u} - v\Omega\cos\varphi)^2 + (\Omega R_\beta \sin\varphi + \dot{v} + u\Omega\cos\varphi + w\Omega\sin\varphi)^2 + (\dot{w} - v\Omega\sin\varphi)^2 \right] AB\mathrm{d}\alpha\mathrm{d}\beta \end{aligned} \quad (21)
$$

where ρ and h are the density and thickness of shell, respectively.

When the composite shell is spinning with a constant rotational speed Ω, centrifugal forces create a stress field that acts like an initial stress in raising natural frequencies. Secondary strain due to circumferential force is as follows [28]:

$$
\begin{aligned}
\varepsilon_\beta^* &= \frac{1}{2}\left(\varepsilon_\beta^{0\,2} + \gamma_{\alpha\beta}^{0\,2} + \phi_\beta^2\right) \\
&= \frac{1}{2}\left[\left(\frac{1}{B}\frac{\partial v}{\partial \beta} + \frac{u}{AB}\frac{\partial B}{\partial \alpha} + \frac{w}{R_\beta}\right)^2 \right. \\
&\quad \left. + \left(\frac{1}{B}\frac{\partial u}{\partial \beta} - \frac{u}{AB}\frac{\partial A}{\partial \beta}\right)^2 + \left(\frac{v}{R_\beta} - \frac{1}{B}\frac{\partial w}{\partial \beta}\right)^2\right].
\end{aligned}
$$

The general expression for the strain energy component due to centrifugal forces is [28]:

$$
U_h = \int_\alpha \int_\beta N_\theta \varepsilon^* AB\,\mathrm{d}\alpha\,\mathrm{d}\beta = \frac{1}{2}\int_\alpha \int_\beta N_\theta \left[\begin{array}{c}\left(\frac{1}{B}\frac{\partial v}{\partial \beta} + \frac{u}{AB}\frac{\partial B}{\partial \alpha} + \frac{w}{R_\beta}\right)^2 \\ + \left(\frac{1}{B}\frac{\partial u}{\partial \beta} - \frac{u}{AB}\frac{\partial A}{\partial \beta}\right)^2 + \left(\frac{v}{R_\beta} - \frac{1}{B}\frac{\partial w}{\partial \beta}\right)^2\end{array}\right]AB\,\mathrm{d}\alpha\,\mathrm{d}\beta \tag{22}
$$

where $N_\theta = \rho h \Omega^2 r(\alpha)^2$, in which r is shown in Fig. 2.

As described above, the ideal boundary conditions are equivalent by using the spring simulation technique, so the boundary potential energy function can be expressed as follows [9]:

$$
U_{\mathrm{spr}} = \frac{1}{2}\int_0^{2\pi}\left\{\begin{array}{c}\left[k_0^u u^2 + k_0^v v^2 + k_0^w w^2 + K_0^w\left(\frac{\partial w}{\partial \alpha}\right)^2\right]_{\alpha=0} \\ + \left[k_L^u u^2 + k_L^v v^2 + k_L^w w^2 + K_L^w\left(\frac{\partial w}{\partial \alpha}\right)^2\right]_{\alpha=L_\alpha}\end{array}\right\}B\,\mathrm{d}\beta. \tag{23}
$$

2.4 Admissible displacement fields

In the vibration mode for the rotating laminated composite shell, the admission displacement components of any circumferential wave number n can be approximated as the following expressions [9]:

$$
\begin{aligned}
u(\alpha,\theta) &= u\cos(n\theta + \omega t) \\
v(\alpha,\theta) &= v\sin(n\theta + \omega t) \\
w(\alpha,\theta) &= w\cos(n\theta + \omega t).
\end{aligned} \tag{24}
$$

In Sect. 2.1, the basic principle of the differential quadrature has been briefly introduced. In this case, it will be directly applied to represent the admission displacement components [24]:

$$
\begin{aligned}
u &= \sum_{i=1}^M l_i(\alpha)\mathbf{U} \\
v &= \sum_{i=1}^M l_i(\alpha)\mathbf{V} \\
w &= \sum_{i=1}^M l_i(\alpha)\mathbf{W}
\end{aligned} \tag{25}
$$

where $l_i(\alpha)$ is the ith Lagrange polynomials. $\mathbf{U}$, $\mathbf{V}$ and $\mathbf{W}$ represent the displacement at Gauss–Lobatto quadrature node of the general shells. Since the Gauss–Lobatto function is obtained in the $(-1,1)$ range, it is necessary to transform the matrix in the differential quadrature method into the solution range corresponding to the size of structure in practical application.

$$
\mathbf{A}_1^{(1)} = \frac{2}{l^e}\mathbf{A}^{(1)} \quad \mathbf{A}_1^{(2)} = \mathbf{A}_1^{(1)}\mathbf{A}_1^{(1)} \quad \mathbf{C}_1 = \frac{l^e}{2}\mathbf{C} \tag{26}
$$

where l^e is the actual size of the structure.

By substituting the above admission displacement functions [Eqs. (24), (25)] into the previous energy functions, the following expressions can be obtained:

$$
U_s = \frac{1}{2}\int_\alpha \pi\left[\begin{array}{c} A_{11}\left(\frac{1}{A}\mathbf{A}_1^{(1)}\mathbf{U} + \frac{1}{R_\alpha}\mathbf{E}\mathbf{W}\right)^2 \\ + 2A_{12}\left(\frac{1}{A}\mathbf{A}_1^{(1)}\mathbf{U} + \frac{1}{R_\alpha}\mathbf{E}\mathbf{W}\right)\left(\frac{1}{AB}\frac{\partial B}{\partial \alpha}\mathbf{E}\mathbf{U} + \frac{n}{B}\mathbf{E}\mathbf{V} + \frac{1}{R_\beta}\mathbf{E}\mathbf{W}\right) \\ + A_{22}\left(\frac{1}{AB}\frac{\partial B}{\partial \alpha}\mathbf{E}\mathbf{U} + \frac{n}{B}\mathbf{E}\mathbf{V} + \frac{1}{R_\beta}\mathbf{E}\mathbf{W}\right)^2 + A_{66}\left(-\frac{n}{B}\mathbf{E}\mathbf{U} + \frac{1}{A}\mathbf{A}_1^{(1)}\mathbf{V} - \frac{1}{AB}\frac{\partial B}{\partial \alpha}\mathbf{E}\mathbf{V}\right)^2\end{array}\right]AB\,\mathrm{d}\alpha \tag{27}
$$

$$U_c = \frac{1}{2}\int_\alpha 2\pi \begin{bmatrix} B_{11}\left(\frac{1}{AR_\alpha}\mathbf{A}_1^{(1)}\mathbf{U} + \frac{1}{A^2}\mathbf{A}_1^{(2)}\mathbf{W}\right)\left(\frac{1}{A}\mathbf{A}_1^{(1)}\mathbf{U} + \frac{1}{R_\alpha}\mathbf{EW}\right) \\ + B_{12}\begin{pmatrix} \frac{1}{ABR_\alpha}\frac{\partial B}{\partial\alpha}\mathbf{EU} + \frac{n}{BR_\beta}\mathbf{EV} \\ + \frac{n^2}{B^2}\mathbf{EW} - \frac{1}{A^2B}\frac{\partial B}{\partial\alpha}\mathbf{A}_1^{(1)}\mathbf{W} \end{pmatrix}\left(\frac{1}{A}\mathbf{A}_1^{(1)}\mathbf{U} + \frac{1}{R_\alpha}\mathbf{EW}\right) \\ + B_{12}\left(\frac{1}{AR_\alpha}\mathbf{A}_1^{(1)}\mathbf{U} + \frac{1}{A^2}\mathbf{A}_1^{(2)}\mathbf{W}\right)\left(\frac{1}{AB}\frac{\partial B}{\partial\alpha}\mathbf{EU} + \frac{n}{B}\mathbf{EV} + \frac{1}{R_\beta}\mathbf{EW}\right) \\ + B_{22}\left(\frac{1}{AB}\frac{\partial B}{\partial\alpha}\mathbf{EU} + \frac{n}{B}\mathbf{EV} + \frac{1}{R_\beta}\mathbf{EW}\right)\begin{pmatrix} \frac{1}{ABR_\alpha}\frac{\partial B}{\partial\alpha}\mathbf{EU} + \frac{n}{BR_\beta}\mathbf{EV} \\ + \frac{n^2}{B^2}\mathbf{EW} - \frac{1}{A^2B}\frac{\partial B}{\partial\alpha}\mathbf{A}_1^{(1)}\mathbf{W} \end{pmatrix} \\ + B_{66}\left(-\frac{n}{B}\mathbf{EU} + \frac{1}{A}\mathbf{A}_1^{(1)}\mathbf{V} - \frac{1}{AB}\frac{\partial B}{\partial\alpha}\mathbf{EV}\right)\begin{pmatrix} -\frac{n}{BR_\alpha}\mathbf{EU} - \frac{1}{ABR_\beta}\frac{\partial B}{\partial\alpha}\mathbf{EV} \\ + \frac{2n}{AB}\mathbf{A}_1^{(1)}\mathbf{W} - \frac{n}{AB^2}\frac{\partial B}{\partial\alpha}\mathbf{EW} + \mathbf{DV} \end{pmatrix} \end{bmatrix} AB d\alpha \tag{28}$$

$$U_b = \frac{1}{2}\int_\alpha \pi \begin{bmatrix} D_{11}\left(\frac{1}{AR_\alpha}\mathbf{A}_1^{(1)}\mathbf{U} + \frac{1}{A^2}\mathbf{A}_1^{(2)}\mathbf{W}\right)^2 \\ + 2D_{12}\left(\frac{1}{AR_\alpha}\mathbf{A}_1^{(1)}\mathbf{U} + \frac{1}{A^2}\mathbf{A}_1^{(2)}\mathbf{W}\right)\begin{pmatrix} \frac{1}{ABR_\alpha}\frac{\partial B}{\partial\alpha}\mathbf{EU} + \frac{n}{BR_\beta}\mathbf{EV}+ \\ + \frac{n^2}{B^2}\mathbf{EW} - \frac{1}{A^2B}\frac{\partial B}{\partial\alpha}\mathbf{A}_1^{(1)}\mathbf{W} \end{pmatrix} \\ + D_{22}\left(\frac{1}{ABR_\alpha}\frac{\partial B}{\partial\alpha}\mathbf{EU} + \frac{n}{BR_\beta}\mathbf{EV} + \frac{n^2}{B^2}\mathbf{EW} - \frac{1}{A^2B}\frac{\partial B}{\partial\alpha}\mathbf{A}_1^{(1)}\mathbf{W}\right)^2 \\ + D_{66}\left(-\frac{n}{BR_\alpha}\mathbf{EU} + \mathbf{DV} - \frac{1}{ABR_\beta}\frac{\partial B}{\partial\alpha}\mathbf{EV} + \frac{2n}{AB}\mathbf{A}_1^{(1)}\mathbf{W} - \frac{n}{AB^2}\frac{\partial B}{\partial\alpha}\mathbf{EW}\right)^2 \end{bmatrix} AB d\alpha \tag{29}$$

$$T = \frac{1}{2}\pi\rho h \int_\alpha \begin{bmatrix} \omega^2\left(\mathbf{U}^2 + \mathbf{V}^2 + \mathbf{W}^2\right) + 2\omega\Omega(\mathbf{VU}\cos\phi + \mathbf{VW}\sin\phi + \mathbf{WV}\sin\phi + \mathbf{UV}\cos\phi) \\ + \Omega^2\left(\mathbf{V}^2 + \mathbf{U}^2\cos^2\phi + \mathbf{W}^2\sin^2\phi + 2\mathbf{UW}\sin\phi\cos\phi\right) \end{bmatrix} AB d\alpha \tag{30}$$

$$U_h = \frac{1}{2}\pi\rho h\Omega^2 \int_\alpha r(\alpha)^2\left[\left(\frac{1}{AB}\frac{\partial B}{\partial\alpha}\mathbf{EU} + \frac{n}{B}\mathbf{EV} + \frac{1}{R_\beta}\mathbf{EW}\right)^2 + \left(\frac{n}{B}\mathbf{EU}\right)^2 + \left(\frac{1}{R_\beta}\mathbf{EV} + \frac{n}{B}\mathbf{EW}\right)^2\right] AB d\alpha \tag{31}$$

$$U_{spr} = \frac{1}{2}\pi \begin{bmatrix} \left(k_0^u\left(\sum_{i=1}^M l_i(0)\mathbf{U}\right)^2 + k_0^v\left(\sum_{i=1}^M l_i(0)\mathbf{V}\right)^2 + k_0^w\left(\sum_{i=1}^M l_i(0)\mathbf{W}\right)^2 + K_0^w\mathbf{A}_{1\,0}^{(1)T}\mathbf{A}_{1\,0}^{(1)}\mathbf{W}^2\right) \\ + \left(k_L^u\left(\sum_{i=1}^M l_i(L)\mathbf{U}\right)^2 + k_L^v\left(\sum_{i=1}^M l_i(L)\mathbf{V}\right)^2 + k_L^w\left(\sum_{i=1}^M l_i(L)\mathbf{W}\right)^2 + K_L^w\mathbf{A}_{1L}^{(1)T}\mathbf{A}_{1L}^{(1)}\mathbf{W}^2\right) \end{bmatrix} B. \tag{32}$$

2.5 Solution method

Based on the above energy expressions, the Lagrangian function of rotating laminated cylindrical, conical and spherical shells with general elastically boundary conditions can be expressed as follows [9]:

$$L = T - U_s - U_c - U_b - U_h - U_{spr}. \tag{33}$$

The equation of motion of the rotating composite shell can be derived using the Hamilton's principle [29], which can be mathematically written as:

$$\frac{d}{dt}\left(\frac{\partial L}{\partial \dot{q}}\right) - \frac{\partial L}{\partial q} = 0 \tag{34}$$

where q is the generalized coordinates $\mathbf{U}$, $\mathbf{V}$ and $\mathbf{W}$.

Through the implementation of Eq. (34), the vibration characteristic equation of the rotating composite shell can be easily obtained. The specific expressions are as follows:

$$\left[\omega^2 \mathbf{M} + \omega \mathbf{G} + \mathbf{K}\right]\mathbf{X} = 0 \tag{35}$$

where

$$\mathbf{M} = \pi \rho h \begin{bmatrix} \mathbf{M}_{uu} & 0 & 0 \\ 0 & \mathbf{M}_{vv} & 0 \\ 0 & 0 & \mathbf{M}_{ww} \end{bmatrix}_{3\times N} AB \tag{36a}$$

$$\mathbf{G} = 2\pi \rho h \Omega \begin{bmatrix} 0 & \mathbf{G}_{uv} & 0 \\ \mathbf{G}_{vu} & 0 & \mathbf{G}_{vw} \\ 0 & \mathbf{G}_{wv} & 0 \end{bmatrix}_{3\times N} AB \tag{36b}$$

$$\mathbf{K} = \mathbf{K}_c + \mathbf{K}_s + \mathbf{K}_b + \mathbf{K}_{spr} + \mathbf{K}_h - \mathbf{M}_h. \tag{36c}$$

For space reasons, the specific expressions of the above matrix elements are given in "Appendix" section. Equation (35) is a nonstandard eigenvalue equation, which can be transformed equivalently into a standard form of eigenvalue equation as follows [15]:

$$\left(\begin{bmatrix} \mathbf{0} & \mathbf{E} \\ -\mathbf{K} & -\mathbf{G} \end{bmatrix} - \omega \begin{bmatrix} \mathbf{E} & \mathbf{0} \\ \mathbf{0} & \mathbf{M} \end{bmatrix}\right)\left\{\begin{matrix} \mathbf{X} \\ \omega \mathbf{X} \end{matrix}\right\} = \mathbf{0}. \tag{37}$$

3 Numerical results and discussion

A unified analytical model for rotating laminated cylindrical shells, conical shells and spherical shells is established. The main purpose of this section is to discuss the numerical results, which mainly contains three research contents: rotating laminated cylindrical shells; rotating laminated conical shells; and rotating laminated spherical shells. According to

the experience of existing literatures, the number of grid points N in this paper is set as 30 for all examples. In order to facilitate the study and comparison, the frequency parameters and rotational speed of the following examples are expressed in the dimensionless form. The specific calculation formulas are as follows: $\omega^* = \omega L\sqrt{\rho/E_2}$ (cylindrical shells), $\omega^* = \omega R_1\sqrt{\rho h/A_{11}}$ (conical shells), $\omega^* = \omega R\sqrt{\rho/E_2}$ (spherical shells) and $\Omega^* = \Omega R\sqrt{(1-\mu^2)/E}$.

3.1 Rotating laminated cylindrical shells

In this subsection, the study of rotating laminated cylindrical shells will be carried out. Table 1 shows the comparison of frequency parameters of non-rotating laminated cylindrical shells with various boundary conditions. In Table 1, the comparative data are from Song et al. [9]. Tables 2 and 3 show the comparison of frequency parameters of rotating laminated cylindrical shells with simply supported and clamped boundary conditions, respectively. ω_b^* and ω_f^* represent non-dimensional frequency parameters of the backward wave and forward wave, respectively. Also, the comparative data in the above tables are from Ref. [9]. The material and geometric parameters of the above tables are defined as follows: $E_2 = 7.6$ GPa, $E_1/E_2 = 2.5$, $G_{12} = 4.1$ GPa, $\mu_{12} = 0.26$, $\rho = 1643$ kg/m^3, $h/R = 0.002$, $L/R = 1$. From Tables 1, 2 and 3, it can be observed that the predicted values by the current method are in good agreement with the existing literature results. Therefore, it indicates that the current method has the ability to predict the vibration characteristics of rotating laminated cylindrical shells under arbitrary elastic boundary conditions.

Next, the parametric studies will be carried out. Figure 5 shows the influence of the circumferential wave number n on the vibration behavior of rotating laminated cylindrical shells with various boundary conditions. In this example, the material and geometric parameters are consistent with those in Table 2. The rotation speed is 20 rev/s. It must be pointed out here that the solid line represents the backward frequencies ω_b^* and the dotted line represents the forward frequencies ω_f^*. In addition, without special explanation, the meanings of dashed and solid lines in all subsequent figures are consistent with those in this figure. Through this study, it can be found that the backward frequency ω_b^* is always larger than the forward frequency ω_f^*. Regardless of the boundary conditions, the frequency parameter always decreases rapidly and then increases gradually with the increase of circumferential wave number n. In addition, when the circumferential wave number n increases and exceeds a certain threshold, the frequency parameters of the rotating laminated cylindrical shells tend to be consistent gradually.

Figure 6 shows the effect of boundary parameters on frequency parameters of rotating laminated cylindrical shells.

Table 1 Frequency parameters ω^* for a three-layered, cross-ply [0°/90°/0°] cylindrical shell with various boundary conditions

Boundary condition	Method	$n=1$	$n=2$	$n=3$	$n=4$	$n=5$	$n=6$
F–F	Ref. [9]	1.115140	1.077907	0.932638	0.782492	0.646864	0.533173
	Ref. [9]	1.152210	1.078821	0.932954	0.782632	0.647052	0.533458
	Present method	1.115139	1.077903	0.932631	0.782480	0.646847	0.533149
C–C	Ref. [9]	1.062242	0.813717	0.629498	0.500864	0.409156	0.341724
	Ref. [9]	1.055098	0.813714	0.629554	0.500832	0.409211	0.341720
	Present method	1.062189	0.813778	0.629498	0.500592	0.408977	0.342301
S–S	Ref. [9]	1.061284	0.804054	0.598331	0.450144	0.345253	0.270754
	Ref. [9]	1.061285	0.804063	0.598337	0.450134	0.345249	0.270759
	Present method	1.061283	0.804051	0.598326	0.450137	0.345244	0.270741

The material parameters and geometric parameters are consistent with Table 2. The boundary condition is defined as setting the spring stiffness of one end to infinity and only changing one type of the spring in the other end at a time. (That is, one varies from 10^{-3} to 10^{11}, while the others are set to 0.) The rotating speed is 20 rev/s. From Fig. 6, it can be found that when the stiffness is 10^4, the frequency parameters do not change. After exceeding this threshold, the change of frequency parameters is related to the type of boundary spring. For example, for rotating spring K^w and linear spring k^u, their changes have little influence on the vibration characteristics of rotating laminated cylindrical shells, while for linear elastic k^v and k^w, their changes have great influence on the vibration characteristics of rotating laminated cylindrical shells. Based on this analysis, two types of elastic boundary conditions are defined: E_1: $k^u=10^8$, $k^v=k^w=K^w=10^{14}$; E_2: $k^v=10^8$, $k^u=k^w=K^w=10^{14}$.

Figure 7 presents the effect of rotation speed on forward and backward frequencies of rotating laminated cylindrical shells with various boundary conditions. The circumferential wave number n is set as $n=1$–3. The material and geometric parameters are consistent with Fig. 6. The dimensionless rotation speed Ω^* varies from 0 to 1. From Fig. 6, it is obvious that when the circumferential wave number n is 1 and 2, the backward frequencies of the laminated cylindrical shells gradually increase with the increase of rotation speed, while the forward frequencies gradually decrease. At that time, when the circumferential wave number is 3, the forward and backward frequencies increase with the increase of rotation speed.

3.2 Rotating laminated conical shells

The main purpose of this section is to carry out the related research of conical shells. Before the parametric studies, some validation work should be carried out first. Table 4 shows the fundamental frequency parameters of an antisymmetric cross-plied laminated conical shell with the S–S

Table 2 Comparison of frequency parameters ω^* for a composite cylindrical shell with two edges simply supported

Ω(rev/s)	n	Ref. [9]		Present method	
		ω_b^*	ω_f^*	ω_b^*	ω_f^*
0.1	3	0.598510	0.598402	0.598471	0.598183
	4	0.450123	0.450084	0.450263	0.450015
	5	0.344932	0.345319	0.345353	0.345140
	6	0.271001	0.270691	0.270839	0.270654
0.4	3	0.598584	0.598091	0.598911	0.597757
	4	0.450396	0.441001	0.450654	0.449660
	5	0.345319	0.345099	0.345714	0.344860
	6	0.271101	0.270801	0.271193	0.270454
1.0	3	0.598992	0.597901	0.599813	0.596930
	4	0.450902	0.449611	0.451502	0.449015
	5	0.346091	0.344991	0.346577	0.344442
	6	0.271901	0.270799	0.272174	0.270326

Table 3 Comparison of frequency parameters ω^* for a composite cylindrical shell with two edges clamped

| Ω(rev/s)	n	Ref. [9]		Present method	
		ω_b^*	ω_f^*	ω_b^*	ω_f^*
0.1	3	0.629596	0.629382	0.629624	0.629349
	4	0.500898	0.500792	0.500951	0.500714
	5	0.409194	0.408993	0.409225	0.4090222
	6	0.341960	0.341692	0.341753	0.341576
0.4	3	0.629795	0.629301	0.630018	0.628919
	4	0.501089	0.500597	0.501329	0.500384
	5	0.408998	0.409101	0.409567	0.408752
	6	0.342106	0.341599	0.342043	0.341333
1.0	3	0.630501	0.628599	0.630911	0.628164
	4	0.501911	0.500392	0.502119	0.499757
	5	0.409889	0.408493	0.410356	0.408320
	6	0.342489	0.341379	0.342960	0.341187
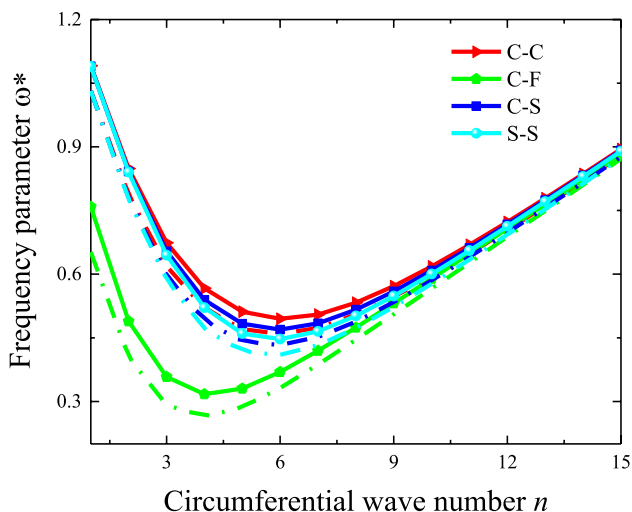
Fig. 5 Variation of the frequency parameter ω^* of a rotating three-layered [0°/90°/0°] cylindrical shell with different circumferential wave numbers n

boundary condition. The numerical results from studies [12, 30, 31] are also given in Table 4 for comparison. Material and geometric parameters are defined as: $\alpha = 30°$, $L^*\sin\alpha/R_1 = 0.25$, $h/R_1 = 0.01, 0.02, 0.03, 0.04, 0.05, 0.06$; $E_1/E_2 = 40$, $G_{12}/E_2 = 0.5$, $\mu_{12} = 0.25$. It can be found that the predicted results of the current method are very close to those from the literature. Because the research on rotating laminated conical shells has not been published in the existing literature, most of them are confined to isotropic materials. Therefore, the next step is to carry out comparative validation of rotating isotropic conical shells. In this paper,
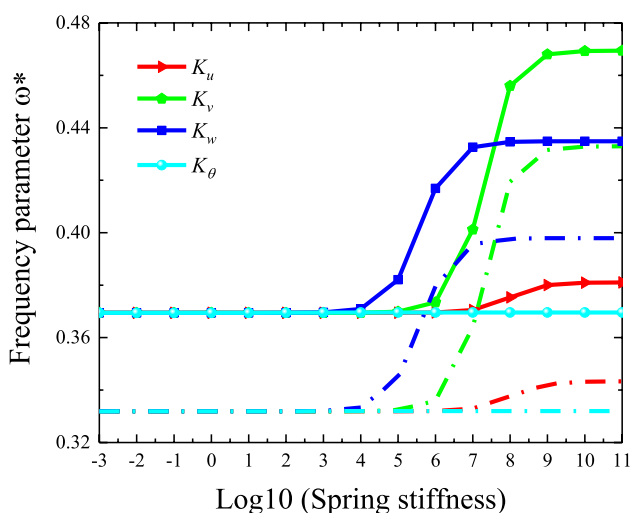

Fig. 6 Frequency for a three-layered [0°/90°/0°] laminated cylindrical shell with one edge clamped, while the other edge restrained by one set of variable stiffness spring

isotropic parameters can be obtained only by setting the following parameters: $E_1/E_2 = 1$, $G_{12} = E_2/2/(1 + \mu_{12})$. Table 5 shows frequency $(m, n) = (1, 1)$ comparisons between the literature results [32] and the present method. Geometric parameters are defined as follows: $\varphi = 30°$, $h/R_0 = 0.01$, $L/R_0 = 6$. By comparison, it can be found that the method in this paper is also accurate in predicting the vibration characteristics of rotating conical shells. Next, some parametric studies will be carried out.

Figure 8 shows the effect of the circumferential wave number n on frequency parameters of three-layered [0°/90°/0°] rotating laminated conical shells with various boundary conditions. In this example, the material and geometric parameters are consistent with those in Table 4. The rotation speed is 20 rev/s. Geometric parameters are defined as follows: $\varphi = 30°$, $h/R_1 = 0.01$, $L/R_1 = 1$. It can be found intuitively that when the circumferential wave number is less than 3, the frequency parameter decreases rapidly with the increase of the circumferential wave number. When the circumferential wave number is more than 3, the frequency parameter increases linearly with the increase of the circumferential wave number. When the wave number is large enough, the frequency parameter tends to be consistent gradually, regardless of the boundary conditions. Figure 9 shows the relationship between boundary parameters and vibration characteristics of three-layered [0°/90°/0°] rotating laminated conical shells. The geometric parameters and material constants are consistent with Fig. 8. The boundary conditions are defined as shown in Fig. 6. It is obvious that the effects of the linear elastic spring k^u and rotating spring K^w on the vibration characteristics of the rotating laminated conical shells are very weak, while the linear elastic springs k^u and k^w are very strong. Figure 10 shows the variation of frequency $(m, n) = (1, 3)$ of three-layered [0°/90°/0°] rotating laminated conical shells subjected to different boundary conditions. In this section, each kind of springs carries one direction with stiffness distributed zero, and the rest springs are assigned infinity. The rotation speed Ω varies from 0 to 20 rev/s. In this example, it can be seen that the backward frequency parameter is always larger than the forward frequency parameter, which is similar to the cylindrical shell. For the backward frequency parameter, the frequency parameter increases with the increase of the rotation speed. However, for the forward frequency parameters, when the rotation speed is less than 5, the forward frequency decreases with the increase of the rotation speed. After the rotation speed is more than 5, the forward frequency parameters gradually increase with the increase of the rotation speed.

3.3 Rotating laminated spherical shells

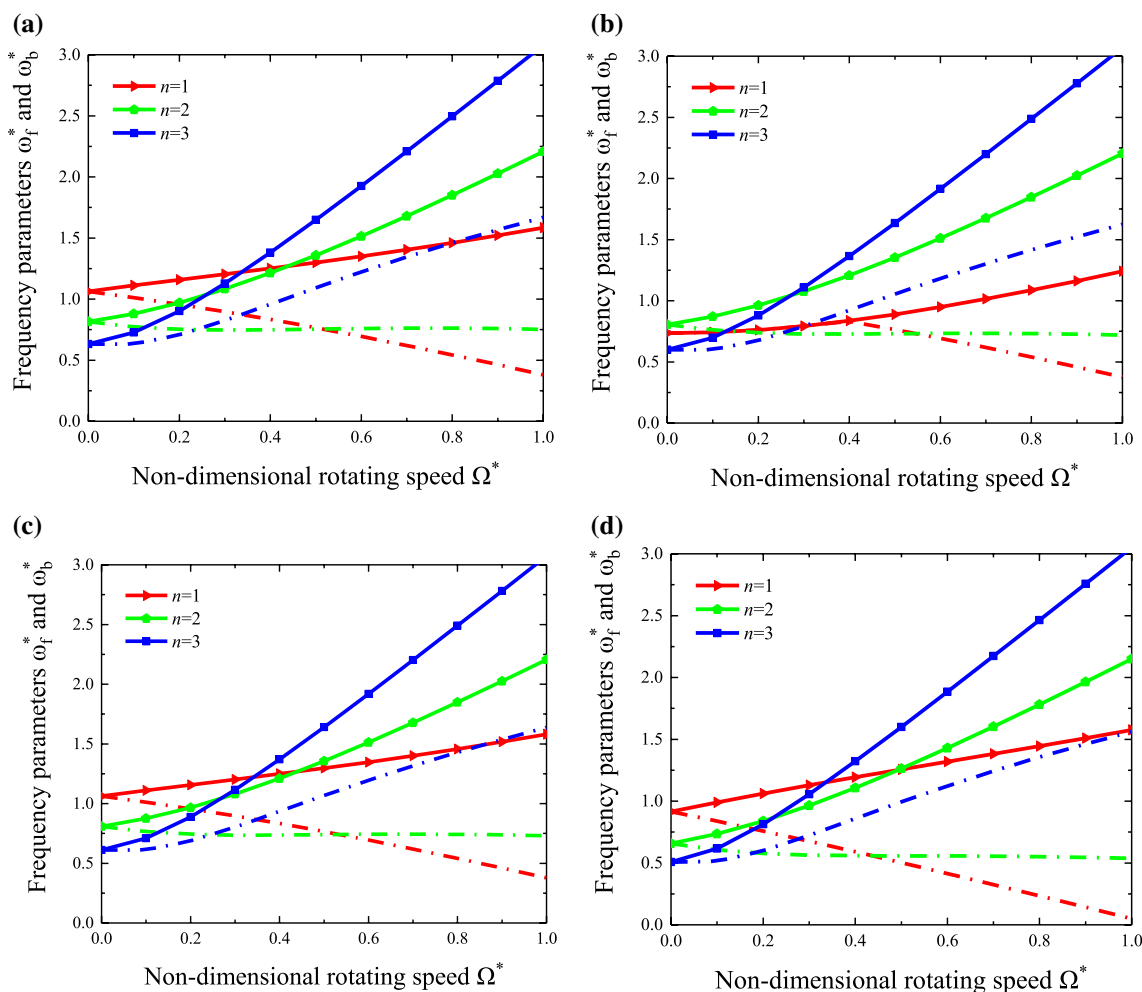Next, the related research work on rotating laminated spherical shells will be carried out. At present, most of the

Fig. 7 Variation of the frequency parameters ω_f^* and ω_b^* of three-layered [0°/90°/0°] laminated cylindrical shell with rotating speed Ω^*: **a** C–C; **b** SD–SD; **c** E1–E1; **d** E2–E2

studies on non-rotating laminated spherical shells are based on the first-order shear deformation theory, and the results of thin laminated spherical shells are lacking. In addition, the research on rotating laminated spherical shells has not been published before. Therefore, in order to verify the correctness of this method, a comparative study between the present method and the finite element numerical results is given here. Table 6 shows the frequency parameters for a non-rotating three-layered [0°/90°/0°] laminated spherical shell. Geometric and material parameters are defined as follows: $\varphi_1 = 60°$, $\varphi_2 = 90°$, $h = 0.01$ m, $R = 1$ m, $E_1 = 138\text{GPa}$, $E_2 = 10.6\text{GPa}$, $G_{12} = 6\text{GPa}$, $\mu_{12} = 0.25$, $\rho = 1500$ kg/m³.

Table 4 Fundamental frequency parameters of an antisymmetric cross-plied laminated conical shell with the S–S boundary condition

h/R_1	Ref. [31]		Ref. [30]		Ref. [12]		Present method	
	With coupling	Without coupling	With coupling	Without coupling	With coupling	Without coupling	With coupling	Without coupling
0.01	0.1769	0.1978	0.1799	0.1976	0.1785	0.1980	0.1770	0.1978
0.02	0.2119	0.2355	0.2153	0.2351	0.2128	0.2353	0.2119	0.2355
0.03	0.2360	0.2671	0.2397	0.2667	0.2402	0.2671	0.2359	0.2671
0.04	0.2578	0.2992	0.2620	0.2987	0.2607	0.2994	0.2577	0.2992
0.05	0.2794	0.3308	0.2841	0.3303	0.2816	0.3307	0.2793	0.3308
0.06	0.3010	0.3606	0.3061	0.3602	0.3024	0.3611	0.3008	0.3606

Table 5 Frequency comparisons between the Han's model and present model with various boundary conditions

Ω^*	Boundary condition	$(m, n) = (1,1)$	Ref. [32]	Ref. [32]	Ref. [32]	Present method
0.2	C–C	ω_f^*	0.6193	0.6021	0.5965	0.5964
		ω_b^*	0.8935	0.8843	0.8831	0.8830
	S–S	ω_f^*	0.5631	0.5366	0.5422	0.5423
		ω_b^*	0.7338	0.7387	0.7248	0.7246
	C–S	ω_f^*	0.5680	0.5414	0.5441	0.5441
		ω_b^*	0.7751	0.7800	0.7624	0.7621
	S–C	ω_f^*	0.6143	0.5956	0.5910	0.5911
		ω_b^*	0.8890	0.8774	0.8767	0.8767
0.3	C–C	ω_f^*	0.5659	0.5268	0.5145	0.5144
		ω_b^*	0.9300	0.9287	0.9403	0.9402
	S–S	ω_f^*	0.4695	0.4371	0.4537	0.4539
		ω_b^*	0.7613	0.7692	0.7619	0.7616
	C–S	ω_f^*	0.5008	0.4412	0.4547	0.4548
		ω_b^*	0.7915	0.7978	0.7974	0.7972
	S–C	ω_f^*	0.5615	0.5210	0.5096	0.5097
		ω_b^*	0.9304	0.9273	0.9362	0.9362

Detailed parameters of the finite element model are as follows: mesh type: S4R (ABAQUS 6.10) and the number of the grid: 30472. By comparing with the results of the finite element method, it can be found that the current method has good calculation accuracy for the study of rotating laminated spherical shells.

Figure 11 shows the correlation between frequency parameters of the rotating three-layered [0°/90°/0°] laminated spherical shells and circumferential wave number n. The rotation speed Ω is 20 rev/s. Obviously, the frequency parameters obtained under fixed boundary conditions are the largest. For C–S boundary and S–S boundary, when the wave number is less than 3, the frequency parameter under S–S boundary is larger than that under C–S boundary, and when the wave number is more than 3, the frequency parameter under S–S boundary is smaller than that under C–S boundary. In addition, the variation of frequency parameters with the wave number is similar to those of cylindrical shells and conical shells. However, it must be noted that no matter how large the wave number is, their frequency parameters do not converge.
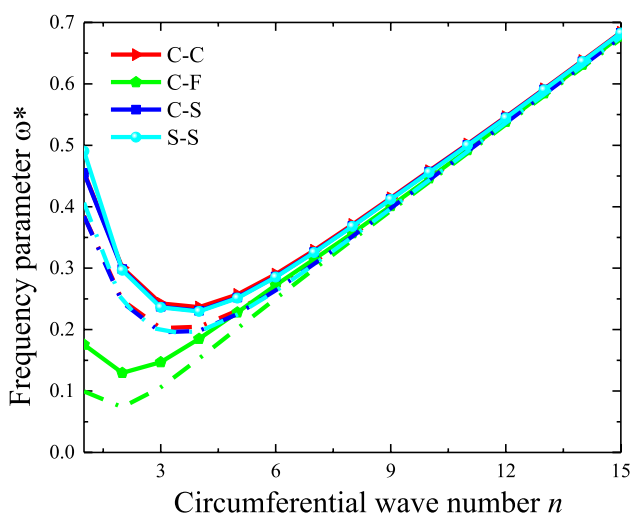

Fig. 8 Variation of the frequency parameters ω^* for a three-layered [0°/90°/0°] laminated conical shell with circumferential wave numbers n
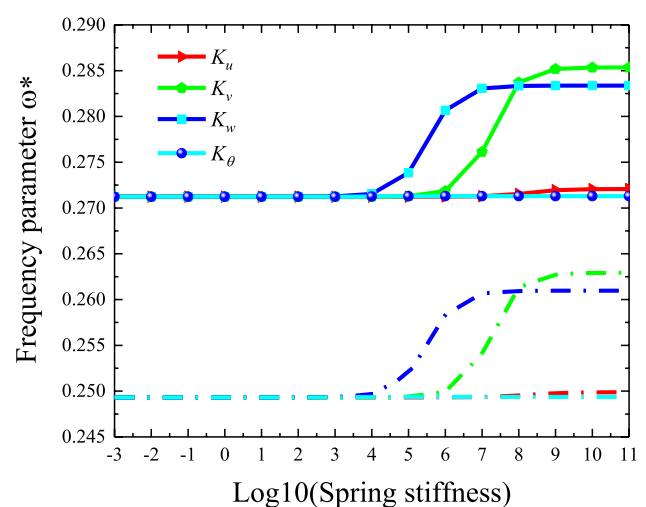

Fig. 9 Frequency for a three-layered [0°/90°/0°] laminated conical shell with one edge clamped, while the other edge restrained by one set of variable stiffness spring

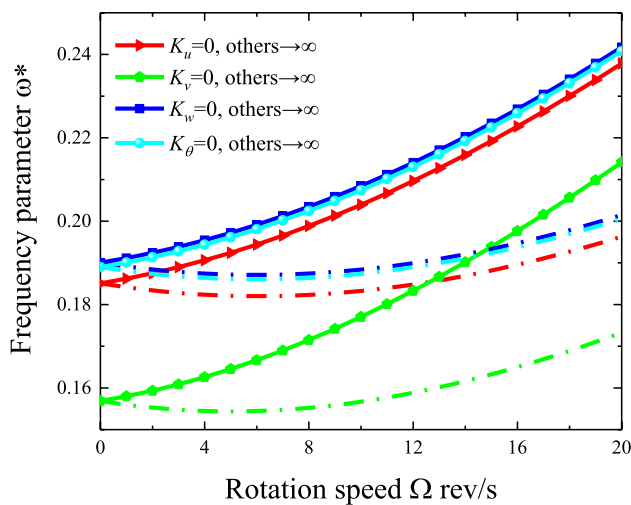**Fig. 10** Vibration of bifurcation of frequency parameter $\omega*$ for a three-layered [0°/90°/0°] laminated conical shell as a function of the rotating speed Ω

Fig. 11 Variation of the frequency parameters $\omega*$ for a three-layered [0°/90°/0°] laminated spherical shell with circumferential wave number n

Figure 12 shows the frequency parameter for a three-layered [0°/90°/0°] spherical shell with elastic boundary conditions. The definition of elastic boundary conditions is consistent with Fig. 6. The material constants and geometric parameters are consistent with Fig. 11. From Fig. 6, it can be found that the stiffness coefficient of the rotating spring K^w has little effect on the vibration characteristics of the rotating laminated spherical shells. However, unlike cylindrical shells and conical shells, the linear spring k^u has the most significant effect on the vibration characteristics of rotating three laminated spherical shells. Figure 13 shows the variation of frequency $(m, n) = (1, 3)$ of rotating three-layered [0°/90°/0°] laminated spherical shells with different rotation speeds. The geometric and material parameters are similar to those in Fig. 12. The definition of boundary conditions is similar to Fig. 10. It is not difficult to find that the frequency parameters of rotating laminated spherical shells are not sensitive to the increase of 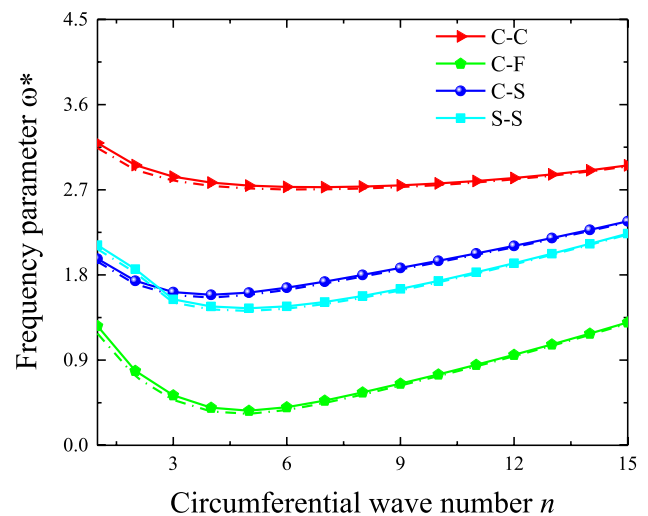the rotation speed. When the rotation speed is less than 6, the frequency parameters are basically unchanged. Therefore, it can be concluded that when the structural form is different, the influence of the same parameters on the vibration characteristics is not consistent.

4 Conclusions

The aim of this paper is to establish a unified analytical model for rotating laminated cylindrical shells, conical shells and spherical shells with various boundary conditions. The Reissner–Naghdi's linear shell theory is adopted to establish the energy function. The spring simulation technique is introduced to simulate general boundary conditions. On the basis of the above, the Lagrangian function of unified rotation laminated shells is established and the differential quadrature is used to represent the displacement function of structure. Finally, the vibration characteristics of the rotating

Table 6 Comparison of frequency parameters $\omega*$ for a composite spherical shell with various boundary conditions

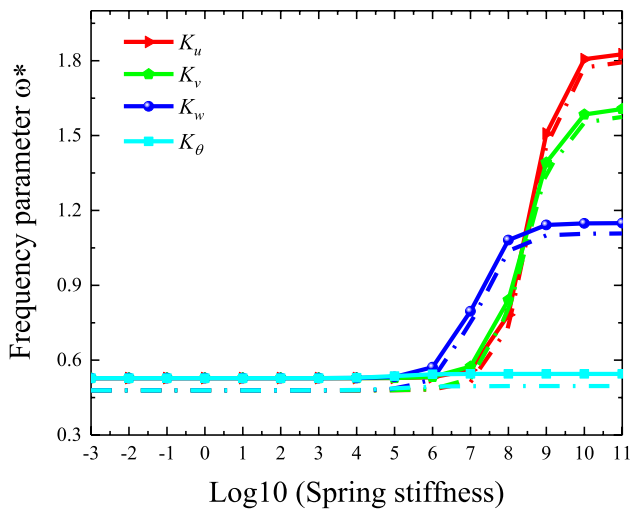| BC	Method	n				
		1	2	3	4	5
F–F	FEM	0.0029	0.0226	0.0643	0.1182	0.1802
	Present method	0.0029	0.0230	0.0649	0.1192	0.1817
F–C	FEM	1.4665	0.9176	0.5967	0.4089	0.3272
	Present method	1.4676	0.9201	0.5986	0.4171	0.3344
C–F	FEM	1.2193	0.7500	0.4865	0.3346	0.2686
	Present method	1.2204	0.7529	0.4901	0.3377	0.2755
C–C	FEM	3.1493	2.9417	2.8462	2.7666	2.7207
	Present method	3.1685	2.9370	2.8408	2.7532	2.7203

Fig. 12 Frequency for a three-layered [0°/90°/0°] laminated spherical shell with one edge clamped, while the other edge restrained by one set of variable stiffness spring
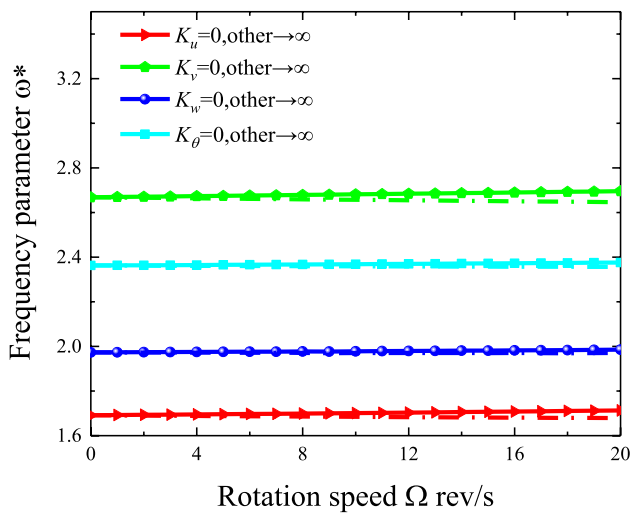

Fig. 13 Vibration of bifurcation of frequency parameter ω^* for a three-layered [0°/90°/0°] laminated spherical shell as a function of the rotating speed Ω

laminated shells will be transformed into a standard system of linear equations. The correctness of the current model is verified by comparing with the existing literature. Considering that the results for rotating laminated conical shells and laminated spherical shells have not been published before, therefore, the work of this paper can be used as reference data for future research.

Compliance with ethical standards

Appendix

$$\mathbf{M}_{uu} = \mathbf{C}\,\mathbf{M}_{vv} = \mathbf{C}\,\mathbf{M}_{ww} = \mathbf{C} \tag{38}$$

$$\mathbf{G}_{uv} = \cos\phi\mathbf{C}\,\mathbf{G}_{vu} = \cos\phi\mathbf{C}\,\mathbf{G}_{vw} = \sin\phi\mathbf{C}\,\mathbf{G}_{wv} = \sin\phi\mathbf{C} \tag{39}$$

$$\mathbf{K}_s = \pi \begin{bmatrix} \mathbf{K}_s^{uu} & \mathbf{K}_s^{uv} & \mathbf{K}_s^{uw} \\ \mathbf{K}_s^{vu} & \mathbf{K}_s^{vv} & \mathbf{K}_s^{vw} \\ \mathbf{K}_s^{wu} & \mathbf{K}_s^{wv} & \mathbf{K}_s^{ww} \end{bmatrix}_{3\times N} AB \tag{40}$$

$$\mathbf{K}_s^{uu} = \frac{A_{11}}{A^2}\mathbf{A}_1^{(1)T}\mathbf{C}\mathbf{A}_1^{(1)} + \frac{A_{12}}{A^2 B}\frac{\partial B}{\partial\alpha}\mathbf{A}_1^{(1)T}\mathbf{C}\mathbf{E}$$
$$+ \frac{A_{22}}{A^2 B^2}\left(\frac{\partial B}{\partial\alpha}\right)^2\mathbf{E}^T\mathbf{C}\mathbf{E} + A_{66}\frac{n^2}{B^2}\mathbf{E}^T\mathbf{C}\mathbf{E} \tag{41}$$

$$\mathbf{K}_s^{uv} = \mathbf{K}_s^{vu} = \frac{nA_{12}}{AB}\mathbf{A}_1^{(1)T}\mathbf{C}\mathbf{E} + \frac{nA_{22}}{AB^2}\frac{\partial B}{\partial\alpha}\mathbf{E}^T\mathbf{C}\mathbf{E}$$
$$- \frac{nA_{66}}{AB}\mathbf{E}^T\mathbf{C}\mathbf{A}_1^{(1)} + \frac{nA_{66}}{AB^2}\frac{\partial B}{\partial\alpha}\mathbf{E}^T\mathbf{C}\mathbf{E} \tag{42}$$

$$\mathbf{K}_s^{uw} = \mathbf{K}_s^{wu} = \frac{A_{11}}{AR_\alpha}\mathbf{A}_1^{(1)}\mathbf{C}\mathbf{E} + \frac{A_{12}}{AR_\beta}\mathbf{A}_1^{(1)}\mathbf{C}\mathbf{E}$$
$$+ \frac{A_{12}}{ABR_\alpha}\frac{\partial B}{\partial\alpha}\mathbf{E}^T\mathbf{C}\mathbf{E} + \frac{A_{22}}{ABR_\beta}\frac{\partial B}{\partial\alpha}\mathbf{E}^T\mathbf{C}\mathbf{E} \tag{43}$$

$$\mathbf{K}_s^{vv} = A_{22}\frac{n^2}{B^2}\mathbf{E}^T\mathbf{C}\mathbf{E} + \frac{A_{66}}{A^2}\mathbf{A}_1^{(1)T}\mathbf{C}\mathbf{A}_1^{(1)}$$
$$- \frac{A_{66}}{A^2 B}\frac{\partial B}{\partial\alpha}\mathbf{A}_1^{(1)T}\mathbf{C}\mathbf{E} + \frac{A_{66}}{A^2 B^2}\left(\frac{\partial B}{\partial\alpha}\right)^2\mathbf{E}^T\mathbf{C}\mathbf{E} \tag{44}$$

$$\mathbf{K}_s^{vw} = \mathbf{K}_s^{wv} = \frac{nA_{12}}{R_\alpha B}\mathbf{E}^T\mathbf{C}\mathbf{E} + \frac{nA_{22}}{BR_\beta}\mathbf{E}^T\mathbf{C}\mathbf{E} \tag{45}$$

$$\mathbf{K}_s^{ww} = \frac{A_{11}}{R_\alpha^2}\mathbf{E}^T\mathbf{CE} + A_{22}\frac{1}{R_\beta^2}\mathbf{E}^T\mathbf{CE} + \frac{A_{12}}{R_\alpha R_\beta}\mathbf{E}^T\mathbf{CE} \tag{46}$$

$$\mathbf{K}_c = \pi \begin{bmatrix} \mathbf{K}_c^{uu} & \mathbf{K}_c^{uv} & \mathbf{K}_c^{uw} \\ \mathbf{K}_c^{vu} & \mathbf{K}_c^{vv} & \mathbf{K}_c^{vw} \\ \mathbf{K}_c^{wu} & \mathbf{K}_c^{wv} & \mathbf{K}_c^{ww} \end{bmatrix}_{3\times N} AB \tag{47}$$

$$\mathbf{K}_c^{ww} = \begin{pmatrix} \frac{B_{11}}{A^2 R_\alpha}\mathbf{A}_1^{(2)T}\mathbf{CE} + \frac{n^2 B_{12}}{B^2 R_\alpha}\mathbf{E}^T\mathbf{CE} - \frac{B_{12}}{A^2 BR_\alpha}\frac{\partial B}{\partial \alpha}\mathbf{A}_1^{(1)T}\mathbf{CE} \\ + \frac{B_{12}}{A^2 R_\beta}\mathbf{A}_1^{(2)T}\mathbf{CE} + \frac{n^2}{B^2 R_\beta}\mathbf{E}^T\mathbf{CE} - \frac{1}{A^2 BR_\beta}\frac{\partial B}{\partial \alpha}\mathbf{E}^T\mathbf{CA}_1^{(1)} \end{pmatrix} \tag{53}$$

$$\mathbf{K}_c^{uu} = \begin{pmatrix} \frac{B_{11}}{A^2 R_\alpha}\mathbf{A}_1^{(1)T}\mathbf{CA}_1^{(1)} + \frac{B_{12}}{A^2 BR_\alpha}\frac{\partial B}{\partial \alpha}\mathbf{E}^T\mathbf{CA}_1^{(1)} + \frac{B_{12}}{A^2 BR_\alpha}\frac{\partial B}{\partial \alpha}\mathbf{A}_1^{(1)T}\mathbf{CE} \\ + \frac{B_{22}}{A^2 B^2 R_\alpha}\left(\frac{\partial B}{\partial \alpha}\right)^2\mathbf{E}^T\mathbf{CE} + \frac{n^2 B_{66}}{B^2 R_\alpha}\mathbf{E}^T\mathbf{CE} \end{pmatrix} \tag{48}$$

$$\mathbf{K}_c^{uv} = \mathbf{K}_c^{vu} = \begin{pmatrix} \frac{nB_{12}}{ABR_\beta}\mathbf{A}_1^{(1)T}\mathbf{CE} + \frac{nB_{12}}{ABR_\alpha}\mathbf{A}_1^{(1)T}\mathbf{CE} + \frac{nB_{22}}{AB^2 R_\beta}\frac{\partial B}{\partial \alpha}\mathbf{E}^T\mathbf{CE} + \frac{nB_{22}}{AB^2 R_\alpha}\frac{\partial B}{\partial \alpha}\mathbf{E}^T\mathbf{CE} \\ - \frac{nB_{66}}{B}\mathbf{E}^T\mathbf{CD} + \frac{nB_{66}}{AB^2 R_\beta}\frac{\partial B}{\partial \alpha}\mathbf{E}^T\mathbf{CE} - \frac{nB_{66}}{ABR_\alpha}\mathbf{E}^T\mathbf{CA}_1^{(1)} + \frac{nB_{66}}{AB^2 R_\alpha}\frac{\partial B}{\partial \alpha}\mathbf{E}^T\mathbf{CE} \end{pmatrix} \tag{49}$$

$$\mathbf{K}_c^{uw} = \mathbf{K}_c^{wu} = \begin{pmatrix} \frac{B_{11}}{AR_\alpha^2}\mathbf{A}_1^{(1)T}\mathbf{CE} + \frac{B_{11}}{A^3}\mathbf{A}_1^{(1)T}\mathbf{CA}_1^{(2)} + \frac{B_{12}}{ABR_\alpha^2}\frac{\partial B}{\partial \alpha}\mathbf{E}^T\mathbf{CE} \\ + \frac{n^2 B_{12}}{AB^2}\mathbf{A}_1^{(1)T}\mathbf{CE} - \frac{B_{12}}{A^3 B}\frac{\partial B}{\partial \alpha}\mathbf{A}_1^{(1)T}\mathbf{CA}_1^{(1)} + \frac{B_{12}}{AR_\alpha R_\beta}\mathbf{A}_1^{(1)T}\mathbf{CE} \\ + \frac{B_{12}}{A^3 B}\frac{\partial B}{\partial \alpha}\mathbf{E}^T\mathbf{CA}_1^{(2)} + \frac{n^2 B_{22}}{AB^3}\frac{\partial B}{\partial \alpha}\mathbf{E}^T\mathbf{CE} - \frac{B_{22}}{A^3 B^2}\left(\frac{\partial B}{\partial \alpha}\right)^2\mathbf{E}^T\mathbf{CA}_1^{(1)} \\ + \frac{1}{ABR_\alpha R_\beta}\frac{\partial B}{\partial \alpha}\mathbf{E}^T\mathbf{CE} - \frac{2n^2 B_{66}}{AB^2}\mathbf{E}^T\mathbf{CA}_1^{(1)} + \frac{n^2 B_{66}}{AB^3}\frac{\partial B}{\partial \alpha}\mathbf{E}^T\mathbf{CE} \end{pmatrix} \tag{50}$$

$$\mathbf{K}_c^{vv} = \begin{pmatrix} \frac{n^2 B_{22}}{B^2 R_\beta}\mathbf{E}^T\mathbf{CE} + \frac{B_{66}}{A}\mathbf{A}_1^{(1)T}\mathbf{CD} - \frac{B_{66}}{A^2 BR_\beta}\frac{\partial B}{\partial \alpha}\mathbf{A}_1^{(1)T}\mathbf{CE} \\ - \frac{B_{66}}{AB}\frac{\partial B}{\partial \alpha}\mathbf{E}^T\mathbf{CD} + \frac{B_{66}}{A^2 B^2 R_\beta}\left(\frac{\partial B}{\partial \alpha}\right)^2\mathbf{E}^T\mathbf{CE} \end{pmatrix} \tag{51}$$

$$\mathbf{K}_b = \pi \begin{bmatrix} \mathbf{K}_b^{uu} & \mathbf{K}_b^{uv} & \mathbf{K}_b^{uw} \\ \mathbf{K}_b^{vu} & \mathbf{K}_b^{vv} & \mathbf{K}_b^{vw} \\ \mathbf{K}_b^{wu} & \mathbf{K}_b^{wv} & \mathbf{K}_b^{ww} \end{bmatrix}_{3\times N} AB \tag{54}$$

$$\mathbf{K}_c^{vw} = \mathbf{K}_c^{wv} = \begin{pmatrix} \frac{nB_{12}}{BR_\alpha R_\beta}\mathbf{E}^T\mathbf{CE} + \frac{nB_{12}}{A^2 B}\mathbf{E}^T\mathbf{CA}_1^{(2)} + \frac{n^3 B_{22}}{B^3}\mathbf{E}^T\mathbf{CE} \\ - \frac{nB_{22}}{A^2 B^2}\frac{\partial B}{\partial \alpha}\mathbf{E}^T\mathbf{CA}_1^{(1)} + \frac{n}{BR_\beta^2}\mathbf{E}^T\mathbf{CE} + \frac{2nB_{66}}{A^2 B}\mathbf{A}_1^{(1)T}\mathbf{CA}_1^{(1)} \\ - \frac{nB_{66}}{A^2 B^2}\frac{\partial B}{\partial \alpha}\mathbf{A}_1^{(1)T}\mathbf{CE} - \frac{2B_{66}}{A^2 B^2}\frac{\partial B}{\partial \alpha}\mathbf{E}^T\mathbf{CA}_1^{(1)} + \frac{nB_{66}}{A^2 B^3}\left(\frac{\partial B}{\partial \alpha}\right)^2\mathbf{E}^T\mathbf{CE} \end{pmatrix} \tag{52}$$

$$\mathbf{K}_b^{uu} = \frac{D_{11}}{A^2 R_\alpha^2} \mathbf{A}_1^{(1)T} \mathbf{CA}_1^{(1)} + \frac{D_{12}}{A^2 B R_\alpha^2} \frac{\partial B}{\partial \alpha} \mathbf{A}_1^{(1)T}$$
$$\mathbf{CE} + \frac{D_{22}}{A^2 B^2 R_\alpha^2} \left(\frac{\partial B}{\partial \alpha} \right)^2 \mathbf{E}^T \mathbf{CE} + \frac{n^2 D_{66}}{B^2 R_\alpha^2} \mathbf{E}^T \mathbf{CE} \tag{55}$$

$$\mathbf{K}_b^{uv} = \mathbf{K}_b^{vu} = \begin{pmatrix} \dfrac{nD_{12}}{ABR_\alpha R_\beta} \mathbf{A}_1^{(1)T} \mathbf{CE} + \dfrac{nD_{22}}{AB^2 R_\alpha R_\beta} \dfrac{\partial B}{\partial \alpha} \mathbf{E}^T \mathbf{CE} \\[2mm] - \dfrac{nD_{66}}{BR_\alpha} \mathbf{E}^T \mathbf{CD} + \dfrac{nD_{66}}{AB^2 R_\alpha R_\beta} \dfrac{\partial B}{\partial \alpha} \mathbf{E}^T \mathbf{CE} \end{pmatrix} \tag{56}$$

$$\mathbf{Ks}_{uu} = k_0^u \left(\sum_{i=1}^{M} l_i(0) \right)^2 + k_L^u \left(\sum_{i=1}^{M} l_i(L) \right)^2 \tag{62}$$

$$\mathbf{K}_b^{uw} = \mathbf{K}_b^{wu} = \begin{pmatrix} \dfrac{D_{11}}{A^3 R_\alpha} \mathbf{A}_1^{(1)T} \mathbf{CA}_1^{(2)} + \dfrac{n^2 D_{12}}{AB^2 R_\alpha} \mathbf{A}_1^{(1)T} \mathbf{CE} - \dfrac{D_{12}}{A^3 B R_\alpha} \dfrac{\partial B}{\partial \alpha} \mathbf{A}_1^{(1)T} \mathbf{CA}_1^{(1)} \\[2mm] + \dfrac{D_{12}}{A^3 B R_\alpha} \dfrac{\partial B}{\partial \alpha} \mathbf{E}^T \mathbf{CA}_1^{(2)} + \dfrac{n^2 D_{22}}{AB^3 R_\alpha} \dfrac{\partial B}{\partial \alpha} \mathbf{E}^T \mathbf{CE} \\[2mm] - \dfrac{D_{22}}{A^3 B^2 R_\alpha} \left(\dfrac{\partial B}{\partial \alpha} \right)^2 \mathbf{E}^T \mathbf{CA}_1^{(1)} - \dfrac{2n^2 D_{66}}{AB^2 R_\alpha} \mathbf{E}^T \mathbf{CA}_1^{(1)} + \dfrac{n^2 D_{66}}{AB^3 R_\alpha} \dfrac{\partial B}{\partial \alpha} \mathbf{E}^T \mathbf{CE} \end{pmatrix} \tag{57}$$

$$\mathbf{K}_b^{vv} = \begin{pmatrix} \dfrac{n^2 D_{22}}{B^2 R_\beta^2} \mathbf{E}^T \mathbf{CE} + D_{66} \mathbf{D}^T \mathbf{CD} - \dfrac{D_{66}}{ABR_\beta} \dfrac{\partial B}{\partial \alpha} \mathbf{D}^T \mathbf{CE} \\[2mm] - \dfrac{D_{66}}{ABR_\beta} \dfrac{\partial B}{\partial \alpha} \mathbf{E}^T \mathbf{CD} + \dfrac{D_{66}}{A^2 B^2 R_\beta^2} \left(\dfrac{\partial B}{\partial \alpha} \right)^2 \mathbf{E}^T \mathbf{CE} \end{pmatrix} \tag{58}$$

$$\mathbf{Ks}_{vv} = k_0^v \left(\sum_{i=1}^{M} l_i(0) \right)^2 + k_L^v \left(\sum_{i=1}^{M} l_i(L) \right)^2 \tag{63}$$

$$\mathbf{K}_b^{vw} = \mathbf{K}_b^{wv} = \begin{pmatrix} \dfrac{nD_{12}}{A^2 B R_\beta} \mathbf{E}^T \mathbf{CA}_1^{(2)} + \dfrac{n^3 D_{22}}{B^3 R_\beta} \mathbf{E}^T \mathbf{CE} - \dfrac{nD_{22}}{A^2 B^2 R_\beta} \dfrac{\partial B}{\partial \alpha} \mathbf{E}^T \mathbf{CA}_1^{(1)} + \dfrac{2nD_{66}}{AB} \mathbf{D}^T \mathbf{CA}_1^{(1)} \\[2mm] - \dfrac{nD_{66}}{AB^2} \dfrac{\partial B}{\partial \alpha} \mathbf{D}^T \mathbf{CE} - \dfrac{2nD_{66}}{A^2 B^2 R_\beta} \dfrac{\partial B}{\partial \alpha} \mathbf{E}^T \mathbf{CA}_1^{(1)} + \dfrac{nD_{66}}{A^2 B^3 R_\beta} \left(\dfrac{\partial B}{\partial \alpha} \right)^2 \mathbf{E}^T \mathbf{CE} \end{pmatrix} \tag{59}$$

$$\mathbf{K}_b^{ww} = \begin{pmatrix} \dfrac{D_{11}}{A^4} \mathbf{A}_1^{(2)T} \mathbf{CA}_1^{(2)} + \dfrac{n^2 D_{12}}{A^2 B^2} \mathbf{A}_1^{(2)T} \mathbf{CE} - \dfrac{D_{12}}{A^4 B} \dfrac{\partial B}{\partial \alpha} \mathbf{A}_1^{(2)T} \mathbf{CA}_1^{(1)} \\[2mm] + \dfrac{n^4 D_{22}}{B^4} \mathbf{E}^T \mathbf{CE} - \dfrac{n^2 D_{22}}{A^2 B^3} \dfrac{\partial B}{\partial \alpha} \mathbf{E}^T \mathbf{CA}_1^{(1)} - \dfrac{n^2 D_{22}}{A^2 B^3} \dfrac{\partial B}{\partial \alpha} \mathbf{A}_1^{(1)T} \mathbf{CE} \\[2mm] + \dfrac{D_{22}}{A^4 B^2} \left(\dfrac{\partial B}{\partial \alpha} \right)^2 \mathbf{A}_1^{(1)T} \mathbf{CA}_1^{(1)} + \dfrac{4n^2 D_{66}}{A^2 B^2} \mathbf{A}_1^{(1)T} \mathbf{CA}_1^{(1)} - \dfrac{2n^2 D_{66}}{A^2 B^3} \dfrac{\partial B}{\partial \alpha} \mathbf{A}_1^{(1)T} \mathbf{CE} \\[2mm] - \dfrac{2n^2 D_{66}}{A^2 B^3} \dfrac{\partial B}{\partial \alpha} \mathbf{E}^T \mathbf{CA}_1^{(1)} + \dfrac{n^2 D_{66}}{A^2 B^4} \left(\dfrac{\partial B}{\partial \alpha} \right)^2 \mathbf{E}^T \mathbf{CE} \end{pmatrix} \tag{60}$$

$$\mathbf{K}_{spr} = \pi \begin{bmatrix} \mathbf{Ks}_{uu} & 0 & 0 \\ 0 & \mathbf{Ks}_{vv} & 0 \\ 0 & 0 & \mathbf{Ks}_{ww} \end{bmatrix}_{3 \times N} B \tag{61}$$

$$\mathbf{Ks}_{ww} = k_0^w \left(\sum_{i=1}^{M} l_i(0) \right)^2 + K_0^w \mathbf{A}_{1\,0}^{(1)T} \mathbf{A}_{1\,0}^{(1)}$$
$$+ k_L^w \left(\sum_{i=1}^{M} l_i(0) \right)^2 + K_L^w \mathbf{A}_{1L}^{(1)T} \mathbf{A}_{1L}^{(1)} \tag{64}$$

$$\mathbf{K}_h = \pi \rho h \Omega^2 \begin{bmatrix} \mathbf{Kh}_{uu} & \mathbf{Kh}_{uv} & \mathbf{Kh}_{uw} \\ \mathbf{Kh}_{vu} & \mathbf{Kh}_{vv} & \mathbf{Kh}_{vw} \\ \mathbf{Kh}_{wu} & \mathbf{Kh}_{wv} & \mathbf{Kh}_{ww} \end{bmatrix}_{3 \times N} AB \tag{65}$$

$$\mathbf{Kh}_{uu} = \frac{1}{A^2 B^2} \left(\frac{\partial B}{\partial \alpha} \right)^2 \mathbf{E}^T \mathbf{C} \mathrm{diag}\left[r(\alpha)^2\right] \mathbf{E} \\ + \frac{n^2}{B^2} \mathbf{E}^T \mathbf{C} \mathrm{diag}\left[r(\alpha)^2\right] \mathbf{E} \tag{66}$$

$$\mathbf{Kh}_{uv} = \mathbf{Kh}_{vu} = \frac{n}{AB^2} \frac{\partial B}{\partial \alpha} \mathbf{E}^T \mathbf{C} \mathrm{diag}\left[r(\alpha)^2\right] \mathbf{E} \tag{67}$$

$$\mathbf{Kh}_{uw} = \mathbf{Kh}_{wu} = \frac{1}{ABR_\beta} \frac{\partial B}{\partial \alpha} \mathbf{E}^T \mathbf{C} \mathrm{diag}\left[r(\alpha)^2\right] \mathbf{E} \tag{68}$$

$$\mathbf{Kh}_{vv} = \frac{n^2}{B^2} \mathbf{E}^T \mathbf{C} \mathrm{diag}\left[r(\alpha)^2\right] \mathbf{E} + \frac{1}{R_\beta^2} \mathbf{E}^T \mathbf{C} \mathrm{diag}\left[r(\alpha)^2\right] \mathbf{E} \tag{69}$$

$$\mathbf{Kh}_{vw} = \frac{n}{BR_\beta} \mathbf{E}^T \mathbf{C} \mathrm{diag}\left[r(\alpha)^2\right] \mathbf{E} + \frac{n}{BR_\beta} \mathbf{E}^T \mathbf{C} \mathrm{diag}\left[r(\alpha)^2\right] \mathbf{E} \tag{70}$$

$$\mathbf{Kh}_{ww} = \frac{1}{R_\beta^2} \mathbf{E}^T \mathbf{C} \mathrm{diag}\left[r(\alpha)^2\right] \mathbf{E} + \frac{n^2}{B^2} \mathbf{E}^T \mathbf{C} \mathrm{diag}\left[r(\alpha)^2\right] \mathbf{E}. \tag{71}$$

The 'diag' represents a diagonal matrix.

$$\mathbf{M}_h = \pi \rho h \Omega^2 \begin{bmatrix} \mathbf{Mh}_{uu} & 0 & \mathbf{Mh}_{uw} \\ 0 & \mathbf{Mh}_{vv} & 0 \\ \mathbf{Mh}_{wu} & 0 & \mathbf{Mh}_{ww} \end{bmatrix}_{3 \times N} AB \tag{72}$$

$$\mathbf{Mh}_{uu} = \cos^2 \phi \mathbf{C} \; \mathbf{Mh}_{uw} = \mathbf{Mh}_{wu} = \sin \phi \cos \phi \mathbf{C}$$
$$\mathbf{Mh}_{vv} = \cos^2 \phi \mathbf{C} \; \mathbf{Mh}_{ww} = \sin^2 \phi \mathbf{C}. \tag{73}$$

References

1. Lam KY, Loy CT (1994) On vibrations of thin rotating laminated composite cylindrical shells. Compos Eng 4(11):1153–1167
2. Hua L, Lam KY (1998) Frequency characteristics of a thin rotating cylindrical shell using the generalized differential quadrature method. Int J Mech Sci 40(5):443–459
3. Lee Y, Kim Y (1998) Vibration analysis of rotating composite cylindrical shells with orthogonal stiffeners. Comput Struct 69:271–281
4. Liew KM, Ng TY, Zhao X, Reddy JN (2002) Harmonic reproducing kernel particle method for free vibration analysis of rotating cylindrical shells. Comput Method Appl M 191(37):4141–4157
5. Saito T, Endo M (1986) Vibration of finite length, rotating cylindrical shells. J Sound Vib 107(1):17–28
6. Civalek Ö, Gürses M (2009) Free vibration analysis of rotating cylindrical shells using discrete singular convolution technique. Int J Pres Ves Pip 86(10):677–683
7. Malekzadeh P, Heydarpour Y (2012) Free vibration analysis of rotating functionally graded cylindrical shells in thermal environment. Compos Struct 94(9):2971–2981
8. Daneshjou K, Talebitooti M (2014) Free vibration analysis of rotating stiffened composite cylindrical shells by using the layerwise-differential quadrature (LW-DQ) method. Mech Compos Mater 50(1):21–38
9. Song X, Zhai J, Chen Y, Han Q (2015) Traveling wave analysis of rotating cross-ply laminated cylindrical shells with arbitrary boundaries conditions via Rayleigh-Ritz method. Compos Struct 133:1101–1115
10. Cai X (1994) Free vibration of a thin rotating shell of revolution. Comput Struct 53(1):155–160
11. Lam KY, Li H (1999) On free vibration of a rotating truncated circular orthotropic conical shell. Compos Part B Eng 30:135–144
12. Civalek Ö (2007) Numerical analysis of free vibrations of laminated composite conical and cylindrical shells: discrete singular convolution (DSC) approach. J Comput Appl Math 205(1):251–271
13. Talebitooti M (2013) Three-dimensional free vibration analysis of rotating laminated conical shells: layerwise differential quadrature (LW-DQ) method. Arch Appl Mech 83:765–781
14. Heydarpour Y, Aghdam MM, Malekzadeh P (2014) Free vibration analysis of rotating functionally graded carbon nanotube-reinforced composite truncated conical shells. Compos Struct 117:187–200
15. Dai Q, Cao Q, Chen Y (2018) Frequency analysis of rotating truncated conical shells using the Haar wavelet method. Appl Math Model 57:603–613
16. Talebitooti M (2018) Thermal effect on free vibration of ring-stiffened rotating functionally graded conical shell with clamped ends. Mech Adv Mater Struct 25(2):155–165
17. Tornabene F (2019) On the critical speed evaluation of arbitrarily oriented rotating doubly-curved shells made of functionally graded materials. Thin Wall Struct 140:85–98
18. Liao SJ (1992) The proposed homotopy analysis technique for the solution of nonlinear problems. PhD thesis Shanghai Jiao Tong University
19. He JH (1999) Variational iteration method—a kind of non-linear analytical technique: some examples. Int J Nonlinear Mech 34(4):699–708
20. Jin C, Wang X, Ge L (2014) Novel weak form quadrature element method with expanded Chebyshev nodes. Appl Math Lett 34:51–59
21. Zhong H, Yue Z (2012) Analysis of thin plates by the weak form quadrature element method. Sci China Phys Mech 55(5):861–871
22. Başhan A (2019) A mixed algorithm for numerical computation of soliton solutions of the coupled KdV equation: finite difference method and differential quadrature method. Appl Math Comput 360:42–57
23. Tong B, Li Y, Zhu X, Zhang Y (2019) Three-dimensional vibration analysis of arbitrary angle-ply laminated cylindrical shells using differential quadrature method. Appl Acoust 146:390–397
24. Guan X, Tang J, Wang Q, Shuai C (2018) Application of the differential quadrature finite element method to free vibration of elastically restrained plate with irregular geometries. Eng Anal Bound Elem 90:1–16
25. Liu B, Ferreira AJM, Xing YF, Neves AMA (2016) Analysis of functionally graded sandwich and laminated shells using a layerwise theory and a differential quadrature finite element method. Compos Struct 136:546–553
26. Jin G, Ye T, Su Z (2015) Structural vibration. Springer, Berlin, Heidelberg
27. Soedel W (2004) Vibrations of shells and plates. Dekker Mechanical Engineering, Hoboken

28. Senjanović I, Alujević N, Ćatipović I, Čakmak D, Vladimir N (2018) Vibration analysis of rotating toroidal shell by the Rayleigh-Ritz method and Fourier series. Eng Struct 173:870–891

29. He JH (2017) Hamilton's principle for dynamical elasticity. Appl Math Lett 72:65–69

30. Shu C (1996) Free vibration analysis of composite laminated conical shells by generalized differential quadrature. J Sound Vib 194(4):587–604

31. Tong L (1994) Free vibration of laminated conical shells including transverse shear deformation. Int J Solids Struct 31(4):443–456

32. Wang J, Cao Y, Lin G (2016) Vibration analysis of high-speed rotating conical shell with arbitrary boundary conditions. Proc Meet Acoust 29(1):065001